



**JOINT STRUCTURES INVOLVING PDSCCS, TCM AND SPACE TIME
CODES**

AHMED AMEER SAEED AL-KATTAN

OCTOBER 2014

**JOINT STRUCTURES INVOLVING PDSCCS, TCM AND SPACE TIME
CODES**

**A THESIS SUBMITTED TO
THE GRADUATE SCHOOL OF NATURAL AND APPLIED
SCIENCES OF
ÇANKAYA UNIVERSITY**

**BY
AHMED AMEER SAEED AL-KATTAN**

**IN PARTIAL FULFILLMENT OF THE REQUIREMENTS FOR THE
DEGREE OF
MASTER OF SCIENCE
IN
THE DEPARTMENT OF
ELECTRONIC AND COMMUNICATION ENGINEERING**

OCTOBER 2014

ABSTRACT

JOINT STRUCTURES INVOLVING PDSCCS, TCM AND SPACE TIME CODES

AL-KATTAN, Ahmed Ameer

M.Sc., Department of Electronic and Communication Engineering

Supervisor: Assoc. Prof. Dr. Orhan GAZI

October 2014, 49 pages

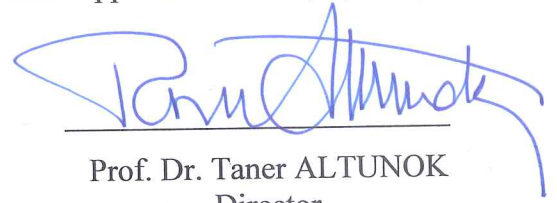
In this thesis we propose new concatenated joint communication structures involving convolutional product codes, space time codes and trellis coded modulation. The first structure consists of convolutional product codes and space time codes. The second one includes convolutional product codes and trellis coded modulation. The proposed structures are all parallel decodable due to the structure of convolutional product codes and have low decoding latencies, which are the main advantages of these proposed structures considering their classical counterparts constructed using serially concatenated convolutional codes, space time codes and trellis coded modulation. The use of multi-antennas at the proposed structures increases the spectral efficiency.

Keywords: Convolutional Product Codes, Space-Time Trellis Codes, Space-Time Block Codes, Trellis Coded Modulation, Decoding Latency, Parallel Processing, Iterative Decoding.

Title of the Thesis : **Joint Structures Involving PDSCCs, TCM and Space Time Codes.**

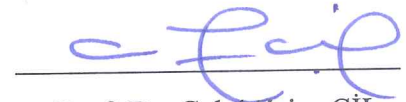
Submitted by **Ahmed Ameer Saeed ALKATTAN**

Approval of the Graduate School of Natural and Applied Sciences, Çankaya University.



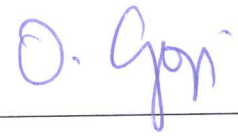
Prof. Dr. Taner ALTUNOK
Director

I certify that this thesis satisfies all the requirements as a thesis for the degree of Master of Science.



Prof. Dr. Celal Zaim ÇİL
Head of Department

This is to certify that we have read this thesis and that in our opinion it is fully adequate, in scope and quality, as a thesis for the degree of Master of Science.



Assoc. Prof. Dr. Orhan GAZİ
Supervisor

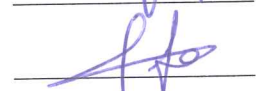
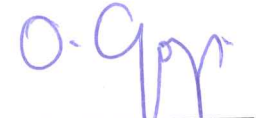
Examination Date: 17.10.2014

Examining Committee Members

Assoc. Prof. Dr. Orhan GAZİ (Çankaya Univ.)

Assoc. Prof. Dr. Fahd JARAD (THK Univ.)

Assist. Prof. Dr. Barbaros PREVEZE (Çankaya Univ.)



STATEMENT OF NON-PLAGIARISM PAGE

I hereby declare that all information in this document has been obtained and presented in accordance with academic rules and ethical conduct. I also declare that, as required by these rules and conduct, I have fully cited and referenced all material and results that are not original to this work.

Name, Last Name : Ahmed Ameer AL-KATTAN

Signature :



Date :

17-10-2014

ÖZ

PÇSBKK, KKM VE UZAY ZAMAN KODLARI İÇEREN YENİ BİRLEŞİK İLETİŞİM YAPILARI

AL-KATTAN, Ahmed Ameer

Yüksek Lisans, Elektronik ve Haberleşme Mühendisliği Anabilim Dalı

Tez Yöneticisi: Doç. Dr. Orhan GAZİ

Ekim 2014, 49 sayfa

Bu tez çalışmasında yeni birleşik iletişim sistemleri önerilmektedir. Önerilen sistemler konvolusyonel çarpım kodları, uzay zaman kodları ve kafes kodlamalı modülasyon içermektedirler. İlk önerilen birleşik sistemin oluşturulmasında konvolusyonel çarpım kodları ile uzay zaman kodları kullanılmıştır. İkinci önerilen sistem ise konvolusyonel çarpım kodları ile kafes kodlamalı modülasyon kullanılarak meydana getirilmiştir. Önerilen sistemler yinelemeli çözüm algoritmaları kullanılarak çözülebilmektedir. Konvolusyonel çarpım kodlarının yapılarından ötürü önerilen sistemler paralel olarak çalışan işlemciler tarafından çözümlenebilmektedir. Bu da çözümüleme esnasında meydana gelen gecikme miktarının klasik birleşik sistemlere göre çok daha az olmasına sebep olmaktadır. Ayrıca çoklu anten kullanımı da spektral verimliliğin üst düzeyde olmasını sağlamaktadır.

Anahtar Kelimeler: Konvolusyonel Çarpım Kodları, Uzay Zaman Kafes Kodlama, Uzay Zaman Blok Kodlama, Kafes Kodlamalı Modülasyon, Çözümüleme Gecikmesi, Paralel İşleme, Yinelemeli Çözüm.

ACKNOWLEDGEMENTS

I would like to express my sincere gratitude to Prof. Dr. Orhan GAZİ for his supervision, special guidance, suggestions, and encouragement throughout the development of this thesis.

It is a pleasure to express my special thanks to my family especially my father Dr. Amer ALKATTAN whose support makes my way of success.

I also would like to express my deepest gratitude to my mother for her support and encouragement and her prayers that make me successful and hopeful in the life.

Finally, I thank Çankaya University Electronic and Communication Engineering Department, for their support.

TABLE OF CONTENTS

STATEMENT OF NON PLAGIARISM.....	iii
ABSTRACT.....	iv
ÖZ.....	v
ACKNOWLEDGEMENTS.....	vi
TABLE OF CONTENTS.....	vii
LIST OF FIGURES.....	x
LIST OF ABBREVIATIONS.....	Xii

CHAPTERS:

1. INTRODUCTION.....	1
1.1. Background.....	1
1.2. Decoding Latency.....	2
1.3. Thesis Organization.....	5
2. CODING THEORY AND CONCATENATED SYSTEMS.....	7
2.1. Channel Coding and Information Theory.....	7
2.2. Error Detection and Correction Codes.....	8
2.2.1. Linear block codes.....	9
2.2.2. Convolutional codes.....	10
2.3. Decoding Algorithm.....	11
2.4. Hard and Soft Decisions.....	12
2.5. Concatenated Codes.....	12
2.6. Turbo Codes.....	13
2.6.1. Parallel concatenated convolutional codes (PCCCs)	13
2.6.2. Serially concatenated convolutional codes (SCCCs).....	15
2.7. Interleaving.....	16
2.7.1 S-Random interleaver.....	17

2.8.	Iterative Decoding.....	17
2.9.	BCJR Algorithm for RSC Codes.....	19
2.10.	Long Domain BCJR Algorithm for RSC Codes.....	21
2.11.	Convolutional Product Codes (CPCs).....	23
2.11.1.	CPCs encoder.....	24
2.11.2.	CPCs decoder.....	25
2.11.3.	CPCs decoding delay.....	26
3.	SPACE TIME CODES AND TRELLIS CODED MODULATION.....	27
3.1.	Introduction.....	27
3.2.	Space Time Trellis Codes.....	27
3.2.1.	Encoding of space-time trellis codes.....	28
3.2.2.	MAP decoding of space-time trellis codes.....	29
3.3.	Space-Time Block Codes.....	29
3.3.1.	Space-time block encoding.....	30
3.3.2.	MAP decoding of space-time block codes.....	31
3.4.	Trellis Coded Modulation.....	32
3.4.1.	Design of trellis coded modulation schemes.....	33
3.4.2.	Set partitioning.....	34
3.4.3.	Selection of the partitions.....	35
4.	LOW LATENCY JOINT COMMUNICATION STRUCTURES.....	37
4.1.	Performance of CPCs, SCCCs, and PCCCs.....	37
4.2.	CPCs Joint Structure with STTCs.....	38
4.2.1.	Symbol to bit prob. / bit. to symbol prob. converter.....	40
4.3.	Joint Structure involving CPCs and STBCs.....	41
4.4.	Joint Structure involving CPCs and TCM.....	43
4.5.	Simulation Results of the Joint Structures.....	44
4.5.1.	Simulation results of CPCs and STTCs.....	44
4.5.2.	Simulation results of CPCs and STBCs.....	45
4.5.3.	Simulation results of CPCs and TCM.....	46

5. CONCLUSION AND FUTURE WORK.....	48
5.1. Conclusions.....	48
5.2. Future Work.....	49
REFERENCES.....	R1
APPENDICES.....	A1
A. CURRICULUM VITAE.....	A1

LIST OF FIGURES

FIGURES

Figure 1	Communication bound for AWGN channel.....	8
Figure 2	Systematic convolutional encoder with code rate $\frac{1}{2}$	10
Figure 3	Systematic convolutional encoder with code rate $\frac{1}{2}$ state diagrams..	11
Figure 4	Non-systematic convolutional encoder with code rate $\frac{1}{2}$	11
Figure 5	Parallel concatenated convolutional encoder.....	14
Figure 6	Parallel concatenated convolutional decoder.....	14
Figure 7	Serially concatenated convolutional encoder.....	15
Figure 8	Serially concatenated convolutional decoder.....	15
Figure 9	Soft-input / soft-output decoding.....	18
Figure 10	Trellis-based computations.....	23
Figure 11	CPCs encoding procedure.....	25
Figure 12	CPCs decoding procedure.....	26
Figure 13	STTC-state encoder with rate $\frac{1}{2}$	28
Figure 14	Transmitter diagram of orthogonal space-time block codes.....	30
Figure 15	Trellis coded modulation procedure.....	33
Figure 16	A constellation diagram (a) Rectangular 16-QAM (b) 8-PSK.....	34
Figure 17	8-PSK set partitioning operation.....	35
Figure 18	TCM with systematic convolutional encoder rate $\frac{2}{3}$	36
Figure 19	Trellis diagram of TCM with systematic convolutional.....	36
Figure 20	PCCC, SCCC and CPC performance graph.....	38
Figure 21	CPCs - STTCs encoding operation.....	39
Figure 22	4-QPSK constellation diagram.....	40
Figure 23	CPCs - STTCs encoding operation.....	41
Figure 24	CPCs - STBCs encoding operation.....	42

FIGURES

Figure 25	CPCs - STBCs decoding operation.....	42
Figure 26	CPCs -TCM encoding procedure.....	43
Figure 27	CPCs - TCMs decoding operation.....	44
Figure 28	CPCs - STTCs and RSCs - STTCs performance graph.....	45
Figure 29	CPCs - STBCs and RSCs - STBCs Performance graph.....	46
Figure 30	8-PSK TCM encoder.....	47
Figure 31	CPCs - TCM and RSCs - TCM Performance graph.....	47

LIST OF ABBREVIATIONS

BCJR	Bahl, Cocke, Jelinek and Raviv
SNR	Signal To Noise Ration
MAP	Maximum A Posteriori
CPCs	Convolutional Code Product Codes
TCM	Trellis Coded Modulation
STTCs	Space-Time Trellis Codes
STBCs	Space-Time Block Codes
PCCCs	Parallel Concatenation Convolutional Codes
SCCCs	Serial Concatenation Convolutional Codes
BW	Bandwidth
AWGN	Additive White Gaussian Noise
BER	Bit Error Rate
SOVA	Soft-Output Viterbi Algorithm
APP	A posteriori Probability
LLR	Long- Likelihood Ratio
RSCs	Recursive Systematic Convolutional Codes
BPSK	Binary Phase Shift Keying
MIMO	Multiple-Input Multiple-Output
SPC	Single Parity Check
QPSK	Quadrature Phase Shift Keying
PSK	Phase Shift Keying
SISO	Soft-Input Soft-Output
STCs	Space-Time Codes
OFDM	Orthogonal Frequency Division Multiplexing
FPGA	Field Programmable Gate Array

CHAPTER 1

INTRODUCTION

1.1. Background

The reliable transmission of information through noisy channels is one of the important requirements of communication systems. In order to design a robust information transmission in the modern communication systems, a powerful channel coding should be applied. Information theory was invented by Shannon in [1]. Shannon stated that it is possible to achieve reliable data transmitting over a communication channel with a lower data rate than the capacity of the channel, if an appropriate error correction codes are used. The researchers are developing error correcting codes to approach Shannon limits for the past sixty years. The first error correcting codes were presented by Hamming and Golay in [2-3]. Hamming and Golay used the same idea, which states that the information block symbols should be divided into sub-blocks with k symbols, then $n-k$ parity symbols should be added to these sub-blocks. The generated code is referred to as a block code and represented by $C(n, k)$. Later on other block codes were developed such as Reed-Muller, cyclic codes, BCH, and Reed Solomon codes [4-5]. Convolutional codes are firstly presented by Elias in [6]. Convolutional codes mix the data and the parity bits uniformly instead of grouping them separately. The encoding operation of the convolutional codes can be performed continuously by using shift registers. These codes became popular and applied in many communication systems after the introduction of the Viterbi algorithm in [7]. For example, GSM standard uses a convolutional code. In [8, 9], the convolutional coding and the modulation processes combined to produce a Trellis coded modulation. Trellis coded modulation is used in the modems and in many satellite communication applications. Trellis coded

modulation is introduced by Ungerboeck. This design provides redundancy required for error control without increasing the signal bandwidth.

Shannon stated that, large coding gain can be achieved by using a long coded sequence, and the researchers attempted to find long codes by using concatenation codes. The earliest research in this field was introduced by Elias in [6]. In this work, two block codes are used sequentially to encode the information frame in order to produce long codes to approach Shannon limit. In 1966 [10], Forney used a soft decision decoding in his concatenation system. After Forney's work, the interest in soft decision decoding and interleaver use increased. For this reason, the researchers consider Forney as the real founder of the concatenated codes.

Turbo codes introduced by C. Berrou, A. Glavieux and P. Thitimajshima were a breakthrough in coding theory [11]. Turbo codes also called parallel concatenation codes. Turbo codes achieve Shannon limit with large codeword lengths. Turbo codes are followed by the serial concatenated convolutional codes and product codes. The good performance of turbo codes lies in the deep knowledge in soft decision algorithm Bahl, Cocke, Jelinek and Raviv (BCJR). It was proved in both empirically and analytically that it was possible to approach the Shannon limits using BCJR algorithm. Turbo codes show a good performance at low SNR values. The major drawback of turbo codes is that they have a large decoding latency due to the complex decoding algorithm and the iterative decoding at the receiver side. Codes with large block size are undesirable because of the large decoding complexity. The maximum a-posterior (MAP) algorithm is employed for decoding purposes. In particular, the real time transmissions like voice and video communications need low latency. For this reason, it is important to find solutions for the high latency problem, since it is clear that the future communication systems will need higher throughput.

1.2. Decoding Latency

In order to alleviate the decoding latency issue, the researchers developed two methods. These methods are complexity reduction for decoding algorithm and parallel processing. The complexity reduction method depends on reducing the

computational processing operations that are needed in decoding algorithm. For complexity reduction method the *M-BCJR* and the *T-BCJR* algorithms were studied in [12]. The *T-BCJR* algorithm has better performance in concatenation structures when it is compared to *M-BCJR* algorithm. Another work related to the complexity of the operation is reducing the number of iterations. This method works by defining good stopping criteria for the iterations if no improvement is seen in the performance of the system. This method is studied in [13-14]. Hence, a number of stopping criteria have been suggested to break the decoding operation as soon as possible if no more performance improvement is seen. Another method to reduce the complexity of decoding is introduced in [15]. In this study, four decoding algorithms are combined in the same decoder. These algorithms are Centre-to-Top, radix-4, early-stop and hard-decision-aided. Early-stop algorithm is used to reduce the number of un-needed iterations. The Radix-4 and Centre-to-Top algorithms involve the concurrent computation of the forward and backward probabilities. For the hard-decision-aided, the outputs of the decoders are compared. If the outputs match, it stops decoding the current block and outputs the hard decision bits.

Multiple processing operations (*Parallel Processing*) are used to obtain higher decoding speed as in [16-17]. In [16-18], the whole trellis stages are divided into multiple overlapped sub-blocks. The same MAP decoders are used for each sub-block. On the other hand, in [17], the trellis is divided into sub-trellises. The multiple processors are utilized in parallel to compute the branch metrics in each sub trellis. In [19], a modified parallel MAP decoder similar to [16-18] is introduced. In this study, instead of employing overlapped sub-blocks the forward and backward probabilities computed in the previous iteration are utilized as a boundary distribution for the next iteration. This method requires additional memory to store the boundary distribution.. The decoding latency is reduced approximately by half when two decoders are run at the same time [20]. However, these methods suffer from performance loss and extra memory usage. Another work is presented to reduce the decoding latency in [21]. An optimized turbo decoder is proposed depending on the sliding-window method in [22]. In this method, Assume that P represents the number of multiple processors and I is the number of iterations. In decoding operation, each processor processes the

entire block for P/I iterations and passes the extrinsic information to the next processor to continue the decoding operation. The decoding latency and the energy consumption are reduced with a small penalty of the area.

Some of channel code families such as block product codes and linear block codes are suitable for parallel processing operation. Product codes are always constructed by linear block codes. Block codes have a trellis structure with a time varying property which makes it unsuitable for implementations. In recent decades, new classes of concatenated codes are proposed which enable parallel processing. These codes are woven turbo codes [24] and convolutional coupled codes [22]. A new structure of product codes based on convolutional codes named as convolutional product codes (CPCs) is introduced in [25]. This class enables parallel processing and uses a different approach than sliding-window technique.

In CPCs structure, the encoder side is parallelized and used directly at the decoder side in order to enable parallel processing operations. Parallelized encoding operation is represented using matrix notation, such that the proposed matrix structure is used to compute the lower and the upper bounds for the worst-case minimum distance of the code. Moreover, the matrix notation helps to determine the number of parallel decoders to guarantee the worst-case minimum distance. CPCs structure can significantly increase the decoding speed in practice. The massive knowledge based for convolutional product codes as what is used exactly in the turbo codes. Due to the advantages of CPCs that mentioned above, this structure is highly suitable to integrate it with some other communication units which have regular trellis structures such as trellis code modulation (TCM), space time trellis codes (STTCs) etc. CPCs have an attractive matrix structure, which makes it suitable for integration with multi-carrier communication. For instance, the vertical dimension utilized for different sub-carriers.

Multi-antenna system techniques are quite important to enhance the performance and the capacity of the system. The use of the multi antenna system was first presented in [27]. Space time coding is used in communication systems to obtain coding gain and

diversity gain. Space time coding is divided into two categories, space time codes (STBCs) and space time trellis codes (STTCs). It is observed that space time trellis codes produce coding gain and diversity gain, the first is not available in space time block codes. Concatenated systems involving STTCs and STBCs were introduced in [28], where iterative decoding is employed for both STTCs and STBCs. In order to obtain coding gain in STBCs, a concatenated structure is proposed in [27]. The concatenated systems of STBCs have decoding complexity that is mainly determined by the outer decoder. On the other hand, the concatenated systems involving STTCs has higher complexity due to trellis based units for both outer and inner decoders. In decoding of both STTCs and STBCs, the complex symbol-wise MAP algorithm is used for iterative decoding. This high complexity creates high decoding delays at the receiver side.

Since, CPCs structure is suitable for parallel processing operations, this make them suitable to integrate with multi antenna systems. In this thesis, we propose and discuss new concatenated communication structures, which involve CPCs and STCs. These proposed structures can be iteratively decoded to make them have high performance, high spectral efficiency due to multi-antenna using, and show low decoding latency.

1.3. Thesis Organization

This thesis consists of five chapters:

Chapter 1 is an introduction and background about the concatenated codes. In addition, the major drawbacks of the turbo codes and the method that is used to reduce the decoding latencies are presented. Finally, the objective of this thesis is presented.

Chapter 2 includes an introduction to channel coding and information theory. Moreover, convolutional encoding and decoding operations are discussed. The iterative decoding and MAP algorithm are explained. The concatenated structures such as PCCCs, SCCC and CPCs are reviewed.

In Chapter 3, a brief introduction to space time codes and trellis coded modulation is made. The encoding and decoding operations of space time trellis codes and space

time block codes are explained. The design of Trellis Coded Modulation Scheme is discussed.

Chapter 4 demonstrates the proposed low latency concatenated structures. The simulation results of these structures are presented and discussed.

Chapter 5 includes conclusions and future work.

CHAPTER 2

CODING THEORY AND CONCATENATED SYSTEMS

2.1. Channel Coding and Information Theory

The In modern communication systems reliable and efficient transmission of the data is an essential issue. The information is mainly transmitted over the noisy and time-variant channel which degrades the performance of the system. Owing to these disturbances, appropriate channel coding schemes have to be utilized such that the error within transmitted data can be detected or corrected. To this end, channel coding theory provides suitable coding schemes for error detection and error correction. Besides, better code characteristics are presented with respect to the number of errors that can be corrected or detected. Coding gain, is defined as the difference in the signal energy between coded and uncoded communication systems to achieve a given bit probability of error. Coding gain is an indicator for the code performance. Nearly 50 years ago Shannon proved that it is possible to transmit the data with low probability of error if codes with very large block lengths are used. After Shannon's theorem channel coding became a very important part of the for modern communication theory. Since the introduction of the Shannon's theorem the researchers are looking for new codes to approach Shannon limits. The capacity formula for the additive white Gaussian noise channel is given as:

$$C = Bw \log(1 + P_s / N_o Bw) \text{ bits/sec.} \quad (2.1)$$

Where C is the capacity of the channel, Bw is the signal bandwidth, P_s is signal power, and N_o is the noise power spectral density. It is seen from (2.1), that if the signal power increases, the capacity of the channel will increase directly. For any

reliable communication the transmission rate (*bits per second*) should be less than the channel capacity as:

$$R < Bw \log(1 + P_s / N_0 Bw) \quad (2.2)$$

Let $\rho = \frac{C}{Bw}$ which is called the spectral efficiency, by using (2.2) and $P_s = R \cdot E_b$. where E_b represents the energy per data bits and R is the rate of the code. The spectral efficiency can be written as:

$$\rho = \log(1 + \rho \cdot E_b / N_o) \quad (2.3)$$

Eq. (2.3) is simplified in order to lead to the following equation:

$$E_b / N_o = 2^\rho - 1 / \rho. \quad (2.4)$$

The previous relation is drawn in Fig. 1, which shows that the reliable communication is possible in the region below the curve. If R approach to zero, $E_b/N_o = \ln 2 \approx -1.6dB$ is the minimum value of E_b/N_o for reliable communication.

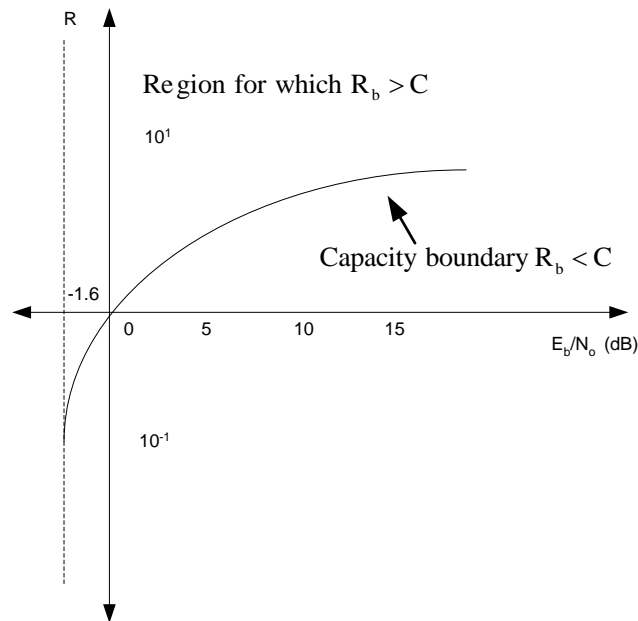


Figure 1 Communication bound for AWGN channel

2.2. Error Detection and Correction Codes

Error detection and correction are techniques that enable the reliable transmission of the digital data over noisy communication channels. Many communication channels are subjected to noise, thus error can occur during transmission. Error detection

techniques allow detecting errors, whereas error correction enables reconstruction of the original data in many cases. In channel coding, redundant bits are added to the data bit stream at the sender and removed by the receiver. The presence of redundant bits allows the receiver to detect or correct the errors. In coding theory, a linear code is considered as an error-correcting code. The linear codes are represented as a vector space [29], where each element of the code is called codeword. Each codeword consists of a sequence of symbols. These symbols are mainly chosen from finite field F , where the code vector is $C = [c_1, c_2, \dots, c_{M-1}, c_M]$, $c_j = [b_1, \dots, b_n]$, $b_i \in F$ for $\forall j, i$. The code rate R is represented as:

$$R = \frac{\log_p(M)}{n}. \quad (2.5)$$

where p is the elements number in the field F . Linear block codes are constructed by adding parity check bits to the end of information bits.

2.2.1. Linear block codes

Linear block codes are a class of parity check codes that can be denoted by the notation (n, k) , where n represents the codeword length and k represents the data length. The encoder transforms block message digits (a message vector) into longer block codeword digits (a code vector). A linear block code is a subspace of the vector space F^n in a finite field F . The total possible number of data-words for k -symbols is equal to V^k where V is the order of the field F . The codewords that are used are equal to V^n . The sets of codewords are chosen carefully considering the Hamming distances among them. The criteria between any codeword pairs is the minimum distance, for this reason, the sets of vectors which have largest minimum distance are chosen to be transmitted. At the receiver side, the Euclidean distance criteria between two codeword pairs are used for vector separation. As long as the Euclidean distance between these codewords becomes larger, better detection and correction of the transmitted codewords can be obtained.

2.2.2. Convolutional codes

Convolutional codes are a type of error-correcting codes. There are two classes of these codes according to the output of the encoders, systematic convolutional and non-systematic convolutional encoders. In systematic classification, the data bits appear directly at the output of the encoder. Whereas in the non-systematic encoder the data bits do not appear at the encoder output. The encoder of convolutional code consists of many shift registers and binary addresses. The number of states in the convolutional encoder is determined by the number of memory cells in the shift registers (M flip-flop). The encoding procedure of the convolutional codes is indicated by using finite state machines which are represented by state diagram, graphs and trellis. The convolutional codes are considered in this thesis are recursive systematic convolutional encoders (*RSCs*) which include a feedback path in the encoder structure as shown in Fig. 2.

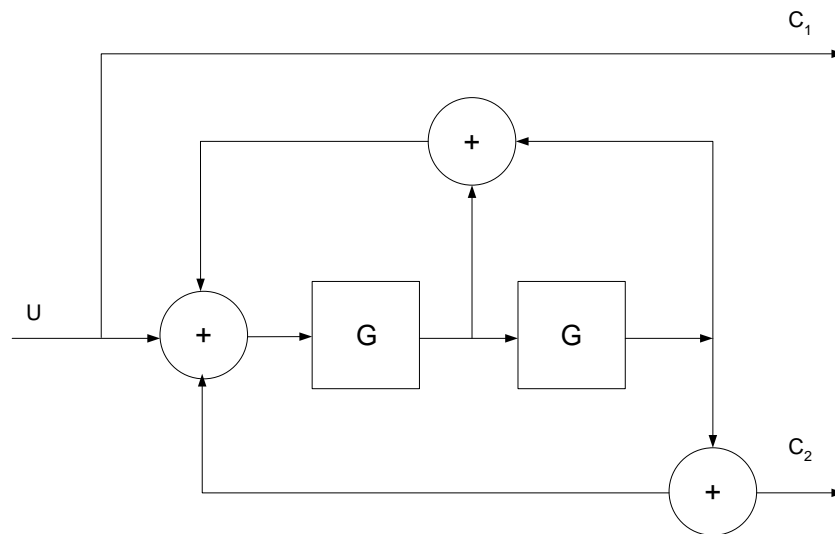


Figure 2 Systematic convolutional encoder with code rate 1/2

The state diagram of the *RSC* for Fig. 2 is depicted in Fig. 3 which fulfills the benefit of the graphical illustration of the state diagram in order to find the transfer function of the convolutional code [24].

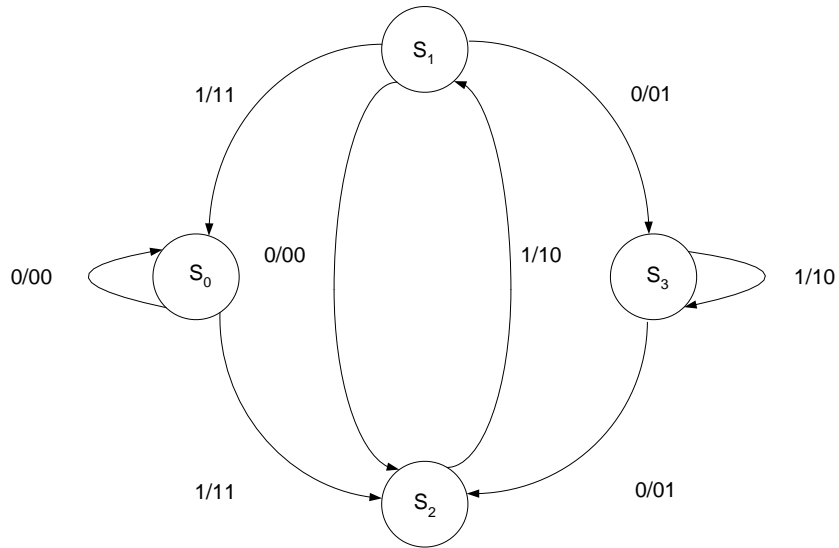


Figure 3 Systematic convolutional encoder with code rate $\frac{1}{2}$ state diagram

The non-recursive systematic convolutional encoder is shown in Fig. 4.

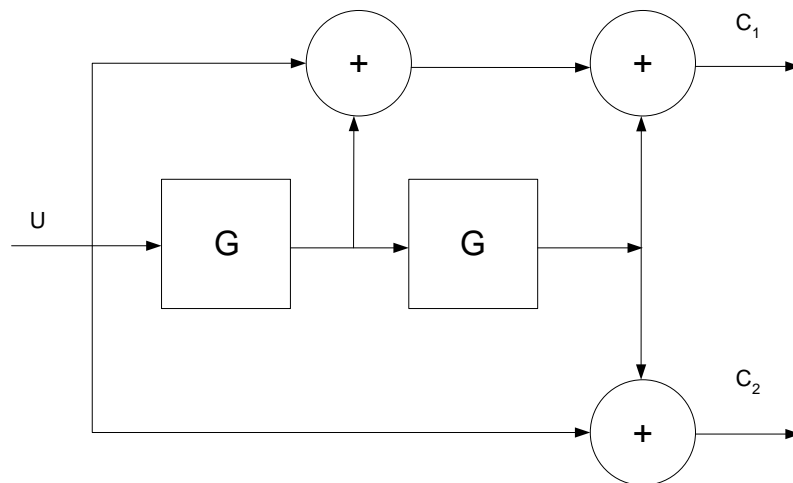


Figure 4 Non-Systematic convolutional encoder with code rate $\frac{1}{2}$

2.3. Decoding Algorithm

The convolutional block codes and linear block codes are decoded using trellis based or algebraic decoding methods. The algebraic techniques have some advantages, the important one is the complexity of decoding is low. However, this method has worse performance than trellis based decoding algorithm. The most famous trellis based algorithms are the maximum *a posteriori* (MAP) and Viterbi algorithms. Both hard and soft decoding techniques are used in Viterbi and MAP algorithms. The Viterbi

algorithm is integrated with the soft decision techniques leading to the soft output Viterbi algorithm (SOVA). Also, MAP algorithm is used for decoding to minimize bit error rate and shows a better performance compared to Viterbi algorithm. In the other hand, the complexity of MAP algorithm is twice of the Viterbi decoding algorithm. The MAP algorithm is modified to log-MAP and max-log-MAP algorithms for practical implementations, which were studied in [30].

2.4. Hard and Soft Decisions

Soft and hard decisions are techniques, which are employed in Viterbi algorithm and MAP algorithm. For instance, if BPSK modulation is used during the communication channel, the 0 bits value is represented as -1 and 1 bit value is represented as 1. When the modulated signal passed through the channel, an AWGN noise is added to the signals. So, the received signals are never been -1 or 1 due to the noise of the channel. In hard decision, a quantizer is used to quantize the received signal to the nearest point in the constellation and an appropriate binary value is assigned. Then the quantized binary sequence is fed to Viterbi decoder. This operation is called hard decision because the decision is made before the decoding operation. In soft decision operation, the quantization is ignored. The received signal values are directly fed to the decoder. Since there is no quantization and demodulation operations applied on the received signal (no hard decision made) for this reason, these values are called soft values. The difference between hard and soft decision is that the former uses soft value in branch metric calculations. Soft decision decoding is used to obtain a good performance near Shannon limit and show a good performance apparently 2 dB better than hard decision.

2.5. Concatenated Codes

Shannon stated that it is possible to obtain reliable transmission over noisy channels if an appropriate error correcting codes are used. In order to achieve Shannon limits, a large codeword block size is used. The construction of these codes with a large size is not difficult task and these codes can achieve a good performance. The decoding

complexity of the generated codes is directly proportional with the size of the codeword. For this reason, the long block length is unaffordable. In order to obtain a large block size, the code concatenation technique has been developed by the researchers. Product codes were introduced by Elias in [27], where short block length codes were combined together to achieve long block length. The next work of Elias is concatenated codes that were presented in [10]. These concatenation systems show high performance and low decoding complexity if they compared to a single code which achieves the same performance. The encoders can be connected in serial or parallel manner or a combination of both to produce the hybrid concatenation.

2.6. Turbo Codes

Turbo codes were introduced in 1993 by C. Berrou, A. Glavieux and P. Thitimajshima represents a breakthrough in coding theory [34]. The general structure of turbo codes consists of two encoders and an interleaver in between. The encoders are always recursive systematic convolutional encoders. The binary data stream is fed directly to the first encoder and the output of the first encoder is passed to the second encoder after being interleaved. The main idea behind turbo codes is the exchange of the extrinsic information between the inner and the outer encoder in a sequential manner. This operation is repeated for a sufficient number of iterations, i.e, typically 8-10 times. The performance of the turbo codes for both parallel and serial concatenation codes is quite close to Shannon limits. The amazing performance of turbo codes was studied in [33], the idea behind this performance was the use of interleaver and the use of MAP algorithm. Many types of interleavers can be used in concatenated systems such as S-random, block, and columns interleaves.

2.6.1. Parallel concatenated convolutional codes (PCCCs)

The structure of the parallel concatenation system consists from two recursive systematic convolutional encoders (RSC) as shown in Fig.5. The overall rate of the code is $\frac{1}{2}$. The input sequence is $U = [u_1, u_2, \dots, u_k]$, where k represents the number of the input sequence. The input data is encoded by using the first encoder to

produce the output sequence p_k . In the second encoder, the input sequence is interleaved before encoding operation. The output of the second encoder q_k is quite different than the output of the first encoder. This means that if one of the output code words has got a low weight, the other usually will have not, and there is a small probability to produce an output with very low weight. The output code sequence of PCCCs is formed by information bits, followed by parity check bits generated by both encoders.

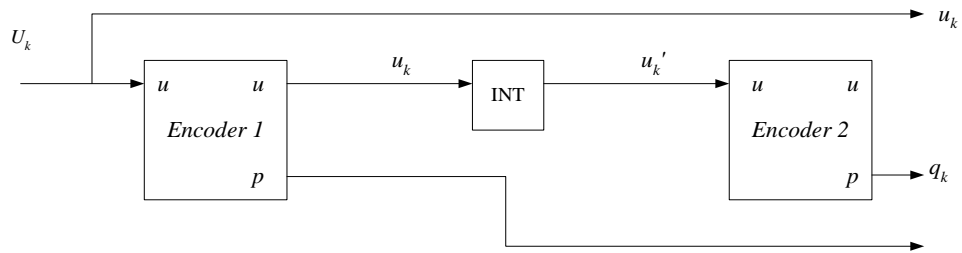


Figure 5 Parallel concatenated convolutional codes encoder

Assume that, the transmitted codewords are $C = [u_1, p_1, q_1, \dots, u_k, p_k, q_k]$. At the receiver side, the received signal is $Y = C + N$ where N represents the noise of the channel, C is the transmitted code. The decoding algorithm that is used in the parallel concatenated systems is soft-input soft-output MAP decoding algorithm. The decoding operation is depicted in Fig. 6.

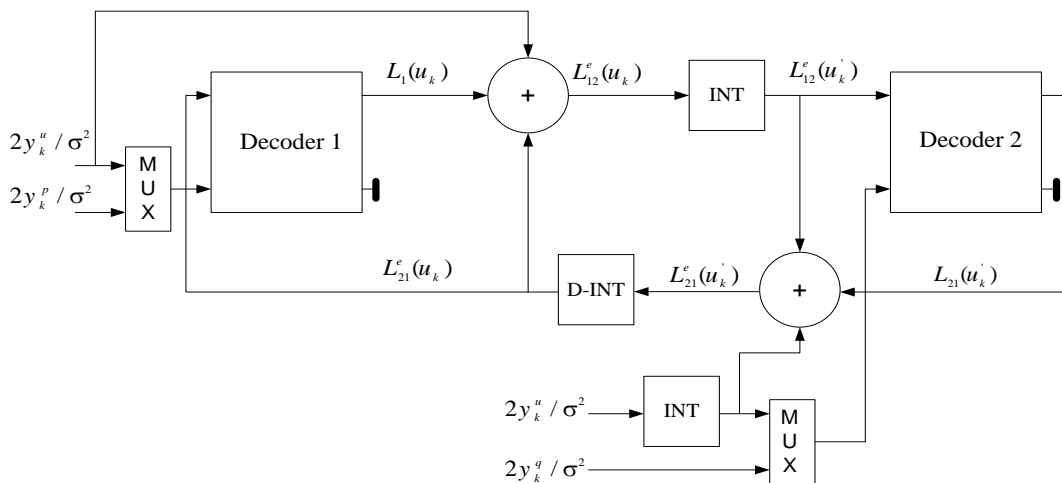


Figure 6 Parallel concatenated convolutional code decoder

2.6.2. Serially concatenated convolutional codes (SCCCs)

The general structure of the serially concatenated codes (SCCCs) consists of two convolutional encoders, inner and outer encoders and an interleaver in between. The input sequence is encoded using the outer encoder and then passed it to the inner encoder after being interleaved. The codewords are transmitted to the channel using single antenna system. The encoding operation of serially concatenated system is depicted in Fig. 7.

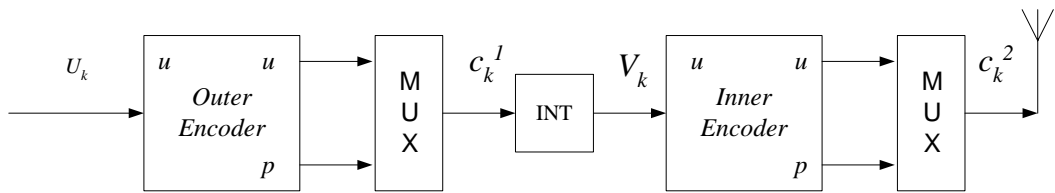


Figure 7 Serially concatenated encoder

The decoding operation of SCCCs codes is a little bit different than a parallel concatenation structure. In SCCCs, the outer decoder calculates the bit probabilities which are used as input coded bit probabilities of the inner decoder. The inner decoder obtains new bit probabilities (updated probabilities) and feeds back to the outer decoder. This operation is repeated for a sufficient number of iterations. The decoding operation is depicted in Fig. 8.

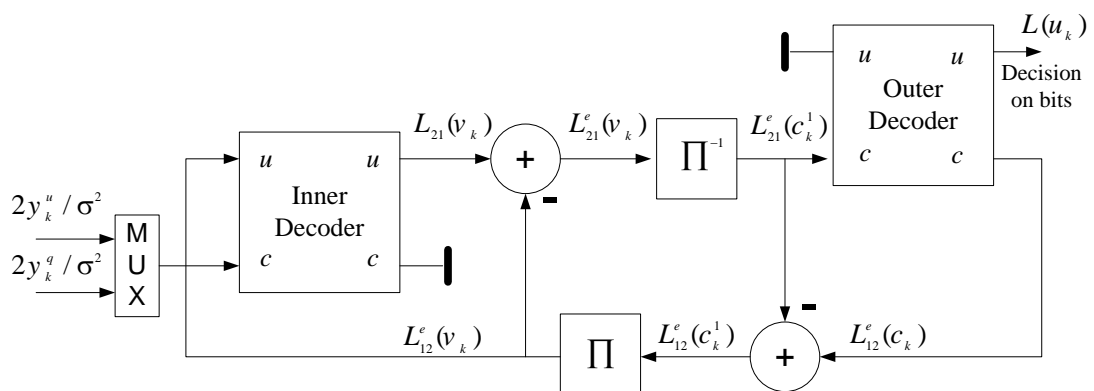


Figure 8 Serially concatenated decoder

2.7. Interleaving

Interleaving is a technique used to improve the forward error correction against burst errors [30]. Interleaving is an operation of re-ordering the data sequence positions. The inverse of the interleaving operation is called de-interleaving. The error correcting capability is enhanced by the use of an interleaver. Interleaving process is very critical for the channels with burst error characteristics. The interleaver is placed between two encoders. At the receiver side, the received signal is de-interleaved, which makes the errors to spread over the time. The interleaver is very important in some concatenated systems that work with iterative decoding. The interleaver is very important in turbo codes, because the interleaver reduces the number of coefficients of low weight codewords. Hereby, the bit error probability is reduced by a factor of $(1/\text{interleaving length})$ which is called interleaving gain [30]. The important roles of the interleaver in the concatenated systems can be outlined as below.

- The input data to the turbo decoders are virtually de-correlated by using an interleaver after performing corrections in the first decoder. There are some uncorrected errors from the first decoder, and these errors can be spread by the interleaver such that the second decoder can correct these errors.
- Interleaver increases the free distance of the codewords and reduces the low weight of the codewords.

There are many interleaves that proposed by the researchers. Each interleaver is designed for specific codes. The Interleavers can be divided into two parts. Block type interleavers and random interleavers. Also, there are many types of block interleavers such as convolutional, shuffle etc. In the random interleavers a pseudo-random operation is involved in their construction. The interleavers have some specifications like causality, delay amount, memory usage etc. The interleaver enhances the performance of the turbo codes. However, some problems arise during the implementation. The common problems of the interleaver in the concatenated

systems are the inefficient use of memory, memory collision, and high hardware complexity.

2.7.1. S-Random interleaver

Spread interleaver is obtained by generating a pseudo-random number from length 1 to N . This kind of interleaver depends on the minimum interleaving distance S , which is defined as [36]:

$$S = \sqrt{\frac{N}{2}} \quad (2.6)$$

The generation of this interleaver can be explained as follows:

Assume an integer sequence of N numbers. A random integer is chosen from the sequence denoted as G_1 . Then the selected element is compared with the previous integer G_2 . If the absolute difference between the selected integer and the previous element is greater than or equal to the distance S , then the element will be accepted otherwise the element will be rejected. The condition of the selection can be defined as:

$$|G_i - G_j| \leq S \quad j=i+1, \dots, S+i \quad (2.7)$$

This interleaver is widely used in turbo codes and other concatenated structures.

2.8. Iterative Decoding

In conjunction with the produced structure of the turbo codes based on a parallel and serial concatenation of two recursive systematic convolutional encoders, a suboptimal decoding scheme depending on iterative decoding is proposed in [34]. The heart of the iterative decoding operation lies on the estimation of the *a posteriori probability* (APPs) $P(u_t|y)$, where u_t represents the t^{th} data bits $t = 1, 2, \dots, T$, and y represents the received codeword with the noise as:

$$y = c + n \quad (2.8)$$

where c represents BPSK modulated signal set $\{\pm 1\}$ and n is AWGN. The knowledge of the APPs allows for optimal decisions on bits u_t via maximum a posteriori (MAP) rule. The decision is made according to:

$$\frac{P(u_t = +1 | y)}{P(u_t = -1 | y)} > 1 \quad (2.9)$$

More suitable expression can be defined as:

$$\hat{u} = \text{sign } L(u_t) \quad (2.10)$$

Where $L(u_t)$ is defined as the *log a posteriori* probability (log-APP) ratio and also called *long-likelihood* which can be defined as:

$$L(u_t) \triangleq \log \left(\frac{P(u_t = +1 | y)}{P(u_t = -1 | y)} \right) \quad (2.11)$$

The SISO decoders consisting of four ports as illustrated in Fig. 9. The SISO decoder receives two log-likelihoods probabilities for input (*information bits*) $L(u_{ik})$ and code $L(c_{ik})$, and then produce the updated log-likelihoods $L(\overline{u_{ik}})$, $L(\overline{c_{ik}})$ the first is also called *extrinsic information*.

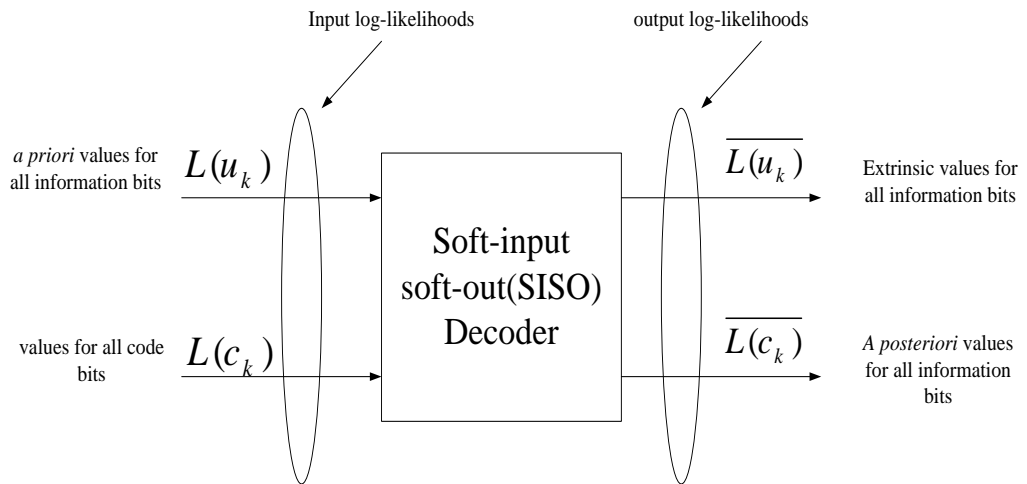


Figure 9 Soft-input/soft-output decoding

Because the SISO decoders compute $L(\overline{u_{it}})$ and $L(\overline{c_{it}})$, the notation $L(M_t)$ is used as temporarily, which represents either u_{ik} or c_{ik} . From Bayes rule, the LLR for an arbitrary SISO decoder is written as follow:

$$L(M_t) \triangleq \log \left(\frac{P(y | u_t = +1)}{P(y | u_t = -1)} \right) + \log \left(\frac{P(u_t = +1)}{P(u_t = -1)} \right) \quad (2.12)$$

Where the second term represents the *a priori* information. Initially, $P(u_k = +1) = P(u_k = -1)$ typically for convolutional decoders. In order to explain the iterative decoding of turbo codes, the PCCC's decoding operation is taken as an example. The PCCC's decoder is illustrated in Fig. 6. The upper encoder and lower encoder are denoted as *encoder1*, *encoder2*, respectively. The decoders are denoted as *decoder1* and *decoder2*, respectively. The decoding iteration proceeds as follows: *Decoder1* receives the extrinsic information from *decoder2* as a priori information after being de-interleaved, in the same manner *decoder2* gets extrinsic information from *decoder1* and the decoding iteration processed between *decoder1* and *decoder2*. The decoding operation is processed as *decoder1* → *decoder2* → *decoder1* → and so on.

2.9. BCJR Algorithm for RSC Codes

This section gives the mathematical description of BCJR algorithm. It is important to know the parameters that are used to in BCJR. Convolutional encoder with rate 1/2 and an AWGN channel are used. A binary phase shift key is used to modulate the signal as $\{1, -1\}$. Let the transmitted codewords vector be denoted as $C = [c_0, c_1, \dots, c_n] = [u_0, p_0, u_1, p_1, \dots, u_n, p_n]$ and $c \triangleq [y_n^u, y_n^p]$. The received signal is written as:

$$Y = C + N \quad (2.13)$$

where the received signal is represented as a vector $Y = [y_1^u, y_1^p, y_2^u, y_2^p, \dots, y_n^u, y_n^p]$. The main goal in BCJR is to compute LLR:

$$L(u_t) \triangleq \log \left(\frac{P(u_t = +1 | y)}{P(u_t = -1 | y)} \right) \quad (2.14)$$

In order to combine the RSC code trellis into this calculation $L(u_t)$ is rewritten as:

$$L(u_t) = \log \frac{\sum_{U^+} p(S_{t-1} = S^-, S_t = S, y)}{\sum_{U^-} p(S_{t-1} = S^-, S_t = S, y)} \quad (2.15)$$

where S_t represents the convolutional encoder state at time t , U^+ and U^- are input pairs for the state transitions from (S_{t-1}, S) to $(S_t = S)$. To simplify (2.17), Bayes rule and mathematical simplifications are used. After simplification the computation of $p(S', S, y) = p(S_{k-1} = S', S_k = S, y)$ is needed for all state transitions and then sums them over the appropriate transitions. The pdf $p(S', S, y)$ is defined as:

$$p(S', S, y) = \alpha_{t-1}(S') \eta_t(S', S) \beta_t(S) \quad (2.16)$$

where the probability $\alpha_t(S)$ is denoted as the forward probabilities which can be computed recursively as:

$$\alpha_t(S) = \sum_{S'} \eta_t(S', S) \alpha_{t-1}(S') \quad (2.17)$$

with initial conditions

$$\alpha_k(s) = \begin{cases} 1, & S = 0 \\ 0, & S \neq 0 \end{cases} \quad (2.18)$$

The probability $\beta_{t-1}(S)$ is denoted as the backward probabilities which can be computed recursively as:

$$\beta_{t-1}(S') = \sum_{S'} \eta_t(S', S) \beta_t(S) \quad (2.29)$$

For the initialization of $\beta_t(S)$, if the code is designed to terminate the trellis at zero state (by adding bits to the end of the data frame) then the initial condition will be:

$$\beta_t(s) = \begin{cases} 1, & S = 0 \\ 0, & S \neq 0 \end{cases} \quad (2.20)$$

The transition probability $\eta_t(S', S)$ is written as follow:

$$\begin{aligned} \eta_t(S', S) &= p(S, y_t | S') \\ &= p(y_t | S', S) p(S | S') \\ &= p(y_t | u_t) p(u_t) \end{aligned} \quad (2.21)$$

where, u_t corresponds to the information bits that causes the transition from $(S_{t-1}, S) \rightarrow (S_t = S)$ and $p(u_t)$ represents the priori probability of these bits. For memoryless AWGN channel $p(y_t | u_t)$ is computed as follow:

$$\eta_t(S', S) = \frac{p(u_t)}{\sqrt{2\pi\sigma}} \exp\left[-\frac{(y_t^u - u_t)^2 + (y_t^p - p_t)^2}{2\sigma^2}\right] \quad (2.22)$$

where $\sigma^2 = N_o/2$. The stable version of the BCJR (long-domain) is presented in the next section.

2.10. Long domain BCJR algorithm for RSC codes

In the log-BCJR algorithm the forward probability $\alpha_t(S)$ is rewritten as follow:

$$\begin{aligned}\bar{\alpha}_t &\triangleq \log(\alpha_t(S)) \\ &= \log\left(\sum_{S'} \eta_t(S', S) \alpha_{t-1}(S')\right) \\ &= \log\left(\sum_{S'} \exp(\eta_t(S', S) + \alpha_{t-1}(S'))\right)\end{aligned}\quad (2.23)$$

With trellis termination assumption the initialization of $\tilde{\alpha}_k(S)$ are done as follow:

$$\tilde{\alpha}_0(s) = \begin{cases} 0, & S = 0 \\ -\infty, & S \neq 0 \end{cases}\quad (2.24)$$

The backward probability $\beta_k(S)$ is calculated as:

$$\begin{aligned}\bar{\beta}_{t-1} &\triangleq \log(\beta_{t-1}(S)) \\ &= \log\left(\sum_{S'} \exp(\eta_t(S', S) + \beta_t(S'))\right)\end{aligned}\quad (2.25)$$

The initialization of $\tilde{\beta}_{t-1}(s)$ under the assumption that the encoders are trellis terminated as follow:

$$\tilde{\beta}_T(s) = \begin{cases} 0, & S = 0 \\ -\infty, & S \neq 0 \end{cases}\quad (2.26)$$

The log-domain calculation of the branch metric is given as:

$$\begin{aligned}\bar{\eta}_t(S', S) &= \log \eta_t(S', S) \\ &= -\log\left(\frac{p(u_t)}{\sqrt{2\pi\sigma}} \exp\left[-\frac{(y_t^u - u_t)^2 + (y_t^p - p_t)^2}{2\sigma^2}\right]\right) \\ &= \log\left(\frac{p(u_t)}{\sqrt{2\pi\sigma}}\right) + \left[-\frac{(y_t^u - u_t)^2 + (y_t^p - p_t)^2}{2\sigma^2}\right]\end{aligned}\quad (2.27)$$

The *LLR* is calculated as follow:

$$\begin{aligned}
L(u_k) &= \log \frac{\sum_{U^+} \alpha_{t-1}(S) \eta_t(S', S) \beta_t(S)}{\sum_{U^-} \alpha_{t-1}(S) \eta_t(S', S) \beta_t(S)} \\
&= \log \left[\sum_{U^+} \exp \left(\tilde{\alpha}_{t-1}(S) + \tilde{\eta}_t(S', S) + \tilde{\beta}_t(S) \right) \right] \\
&\quad - \log \left[\sum_{U^-} \exp \left(\tilde{\alpha}_{t-1}(S) + \tilde{\eta}_t(S', S) + \tilde{\beta}_t(S) \right) \right] \tag{2.28}
\end{aligned}$$

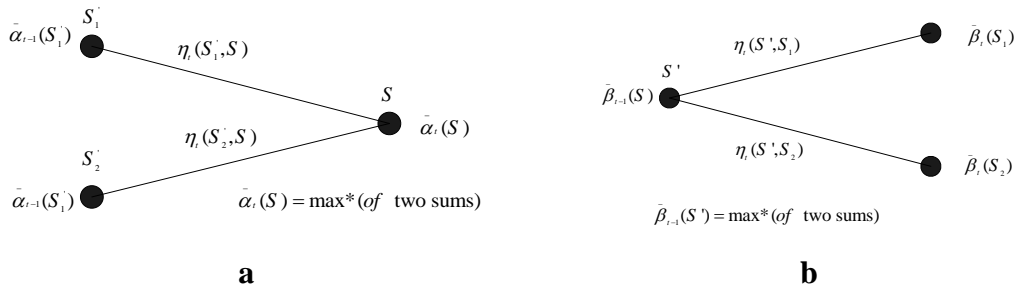
After many mathematical operations and using $\max^*(\cdot)$ Function the forward, backward and LLR probabilities and is rewritten as:

$$\tilde{\alpha}_t(S) = \max_{S'}^* \left(\tilde{\alpha}_{t-1}(S') + \tilde{\eta}_t(S', S) \right) \tag{2.29}$$

$$\tilde{\beta}_t(S) = \max_{S'}^* \left(\tilde{\beta}_t(S') + \tilde{\eta}_t(S', S) \right) \tag{2.30}$$

$$\begin{aligned}
L(u_k) &= \max_{U^+}^* \left[\tilde{\alpha}_{t-1}(S) + \tilde{\eta}_t(S', S) + \tilde{\beta}_t(S) \right] \\
&\quad - \max_{U^-}^* \left[\tilde{\alpha}_{t-1}(S) + \tilde{\eta}_t(S', S) + \tilde{\beta}_t(S) \right] \tag{2.31}
\end{aligned}$$

Fig. 10, Shows pictorially the trellis-based calculations in Eqs. (2.29), (2.30) and (2.31). Also, it is seen from the previous three equations, how the long domain computation is vastly simplified relative to the probability domain computation. The $\max^*(\cdot)$ function involves two terms $\max(\cdot)$ function and one correction terms which is $\log(1 + e^{-|x-y|})$.



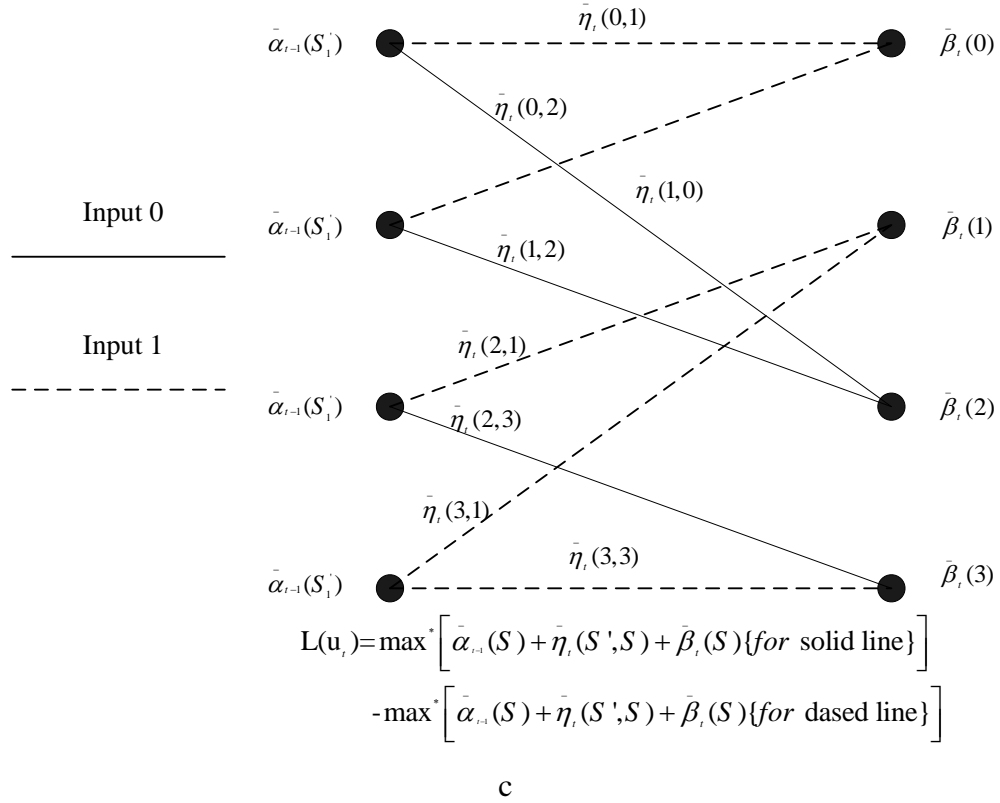


Figure 10 Trellis-based computations.

(a) Shows The Forward recursion in Eq. (2.29). (b) Shows the backward recursion in Eq. (2.30). (c) Shows the computation of $L(u_i)$ in Eq. (2.31).

2.11. Convolutional Code Product (CPCs)

The goal of concatenated codes is to build a robust error correcting code with lower decoding complexities. In 1966 Forney [10] introduced concatenated codes. Turbo codes (parallel concatenation) received a huge interest after the introduction to iterative decoding. Turbo codes achieve a bit error rate (BER) levels around 10^{-5} at low SNR values close to Shannon's limit. The key behind the success and good performance of turbo codes was the use of the soft-in soft-out decoding algorithms. Parallel concatenated convolutional codes lead to the development of serially concatenated convolutional codes in [34], which showed better performance than PCCCs. However, their height decoding latency reduces their attractiveness for practical implementations.

Single parity check (SPC) product codes are studied in [37]. Product codes are very simple and have low complexity code. Although product codes have high decoding latency due to the complexity of decoding algorithm, they are highly suitable for parallel processing. Turbo product codes based on convolutional codes are studied in [25]. Convolutional codes are used in this structure due to the time-invariant of the trellis structure, which makes them more convenient for implementation. In addition, another technique such as trellis coded modulation can be integrated with this structure.

2.11.1. CPCs encoder

The input data/symbol sequence is put into a matrix. Each row of the data matrix is encoded using linear block or recursive systematic convolutional codes (*RSCs*), although other codes can be used for encoding. Then the encoded matrix is converted to the serial sequence to be interleaved. The interleaved sequence is converted to a matrix to obtain the interleaved matrix. The interleaved matrix columns are encoded separately using the same encoders. The encoded matrix is converted to a single vector. The vector is BPSK modulated then transmitted using a single antenna. The encoding operation is seen in Fig.11, where recursive systematic convolutional codes are used for encoding the rows and the columns.

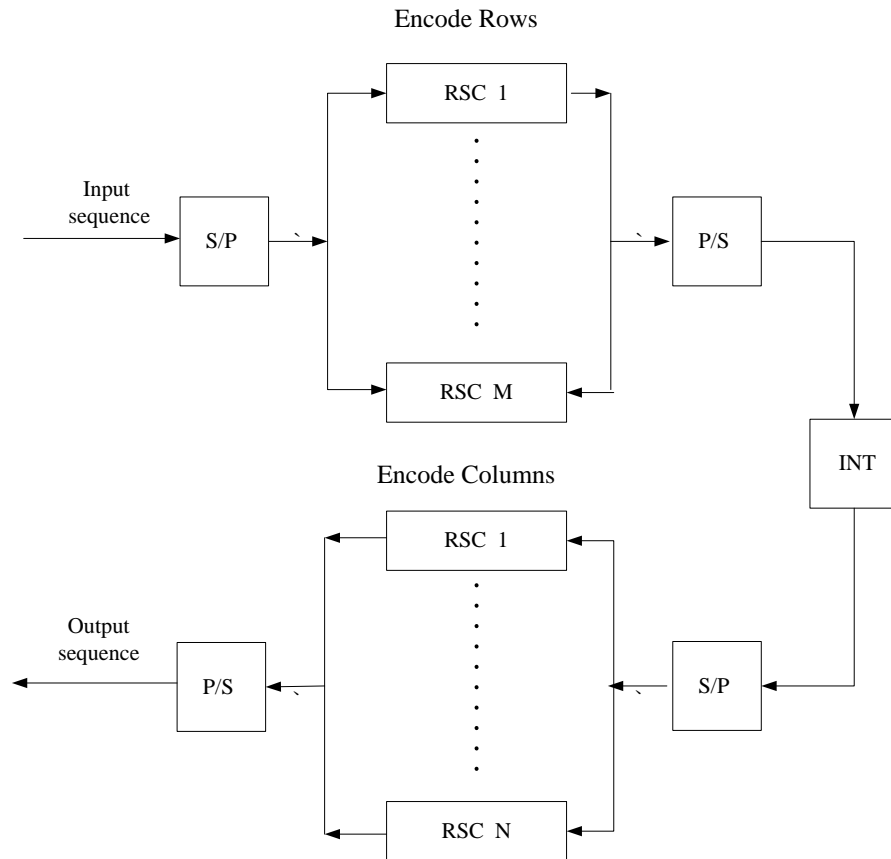


Figure 11 CPCs encoding procedure

The modulated signal is passed through an additive white Gaussian noise (AWGN) channel. The use of interleaver is very critical for this structure. A good performance will be obtained if an effective interleaver is used.

2.11.2. CPCs decoder

For the decoding operation, separated log-MAP decoders are utilized for each row and columns. The columns are decoded individually using log-MAP decoders. The extrinsic information that obtained from columns decoders is passed to de-interleaver. Then the de-interleaved extrinsic information is passed to the row decoders, which are decoded via independent log-MAP decoders. This process is repeated for a sufficient number of iterations. The whole decoding operation is depicted in Fig. 12.

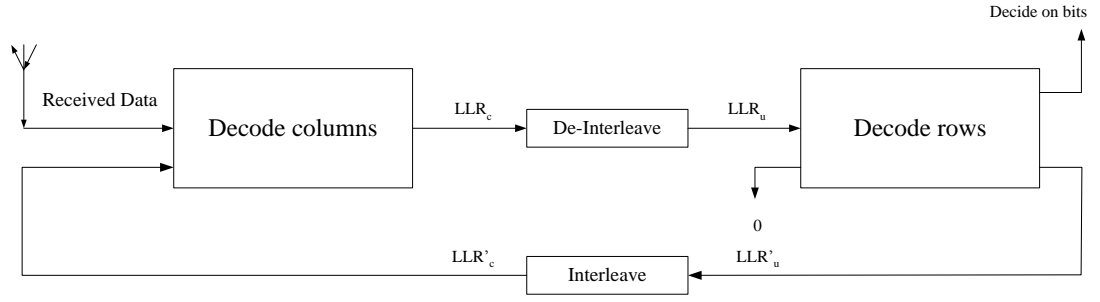


Figure 12 CPCs decoding procedure

2.11.3. CPCs decoding delay

The decoding structure of CPCs provides advantages and implementations for practical systems. In other words, assume the received vector with length L . Let C be the computational complexity and T is the latency of a single stage of trellis code. In *SCCCs* decoding, two log-MAP decoders are employed. The inner decoder has a complexity with order $O(C * 2L)$ and time delay $O(T * 2L)$ due to the long input sequence. The outer decoder has a complexity of $O(C * L)$ and time delay of $O(T * L)$. The overall decoding complexity of *SCCCs* is $O(C * 3L)$ and time delay is $O(T * 3L)$. On the other hand, the CPCs use separated log-MAP decoders for each row and column in decoding operation. Assuming that $N=M$ represents the number of rows and columns decoded. In CPC columns are decoded first the use of the separate log-MAP decoders for each row and column makes parallel processing operations possible. Each column decoder has complexity $O(\sqrt{L})$ and the time delay (\sqrt{L}) . Since these decoders are run in parallel the total column decoding complexity is of $O(2L)$ but the time delay is (\sqrt{L}) . Similarly, row decoding has a total complexity of $O(L)$ and time delay $O(\sqrt{L})$. Hereby, the decoding time delay is reduced by the factor N due to the parallel processing while keeping the same computational complexity. Certainly, the decoding latency is decreased by using multi processors working at the same time. This results in the increment in hardware.

CHAPTER 3

SPACE TIME CODES AND TRELIS CODED MODULATION

3.1. Introduction

In the last years, there was a huge growing demand for higher data rates in communication systems such as cellular networks, wireless local area networks and video broadcasting. In order to meet the demand for high data rates, multi antenna should be used in the transmitter and receiver. The use of multi antenna in the transmitter and receiver creates multiple-input multiple-output (MIMO) channel. MIMO channel not only offers higher transmission rates, it can also enhance the system reliability and robustness to noisy channel comparing it to the single antenna systems. The main advantages of the MIMO system are beamforming, spatial diversity and spatial multiplexing. If space time codes are used in multi antenna communication systems, coding gain can also be obtained in addition to the diversity. New techniques of codes called space-time codes are proposed by Tarokh Seshadri and Claderbank in [26]. Another technique of space-time codes called space-time block codes were developed by Alamouti [38].

3.2. Space-Time Trellis Codes

Space-time trellis codes (STTCs) are formed by a method that combines modulation and trellis coding at the transmitter side to transmit and receive data over multiple antenna channel. The main task of the space-time trellis code is to achieve coding gain and full diversity. The rate of STTCs is defined as the number of transmitted symbols per time slot. MAP or Viterbi algorithms are used to recover the received

signal. There are different designs of space-time trellis codes for 8-PSK, QPSK and 16-QAM.

3.2.1. Encoding of space-time trellis codes

Consider a mobile communication system with N transmitted antennas and M received antennas. Space-time trellis codes are represented by a trellis and pair of symbols for each trellis path. The STTCs send R bits/(s Hz) of data. There are 2^b branches leave every state at time instance t . A set of 2^b pair refers to the next every state represented as 2^b pairs of symbols for the 2^b leaving branches from top to bottom. For instance, Tarokh's 4-state STTC state diagram is depicted in Fig.13.

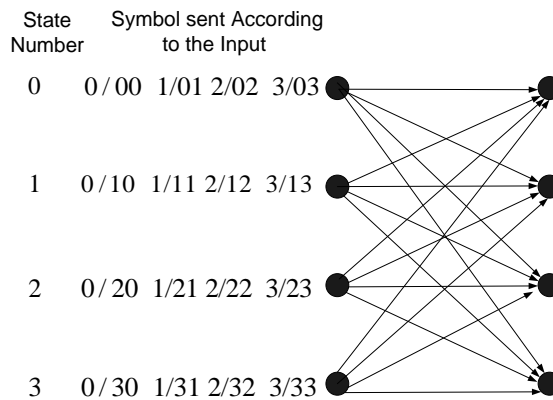


Figure 13 STTC 4-state encoder with Rate 1/2.

This scheme uses two transmitter and receiver antennas. The encoding operation is explained as follows:

The input bits stream is QPSK mapped and represented as S_0, S_1, S_2, S_3 . Then, the modulated signal is sent to the state machine, the parity symbols are added to the original symbols. For example, lets the initial state be 0. An input symbol with a number S_2 enters to the state machine. Next, the symbols that are numbered with S_2 and S_1 are transmitted from antenna number (1, 2) and a transition from state 0 to 1 occurs.

3.2.2. MAP decoding of space-time trellis codes

Space-time trellis codes are decoded using Viterbi or symbol-wise MAP algorithms. In symbol-wise MAP algorithm the transition probability $\gamma(s, \hat{s})$ for any number of transmitted antennas M and received antennas N is calculated as follow:

$$\eta(s, \hat{s}) = e^{-\left[\sum_{i=1}^M \left| y_i - \sum_{j=1}^N h_{ij} s_j \right|^2 \right] / 2\sigma^2} \quad (3.1)$$

where, y represents the received signal corresponding to the antenna, $h_{i,j}$ are the channel coefficients between the transmitter i and receiver j , S_j is the transmitted symbol from transmit antenna j and is determined from the state transition diagram of the STTCs. The transitions probabilities are used to recursively compute the value of forward and backward probabilities. The forward probability $\alpha_{t-1}(\hat{s})$ is computed recursively as:

$$\alpha_t(s) = \sum_{\text{all } \hat{s}} \gamma_t(\hat{s}, s) \alpha_{t-1}(\hat{s}) \quad (3.2)$$

And the values of backward probabilities $\beta_t(s)$ are computed recursively as:

$$\beta_{t-1}(s) = \sum_{\text{all } \hat{s}} \eta_t(\hat{s}, s) \beta_t(\hat{s}) \quad (3.3)$$

Finally the APP is obtained as follow:

$$LLR(s) = \sum_{\text{all } \hat{s}} \eta_t(\hat{s}, s) \beta_t(\hat{s}) \alpha_{t-1}(\hat{s}) \quad (3.4)$$

3.3. Space-Time Block Codes

Space-time trellis codes show a good performance at the cost of relatively high decoding complexity. In [37] Alamouti proposed a remarkable scheme for the transmission using two antennas. A simple decoding algorithm was presented by Alamouti in [37]. This algorithm is generalized to an arbitrary number of received antennas. The Alamouti scheme that uses two transmitter antennas is less complex than space-time trellis codes, however, there is a loss in performance [38] due to the lack of coding gain.

3.3.1. Space-time block encoding

Fig. 14, shows the classical block diagram of space-time block encoder. There are two categories of Alamouti code, two transmitter and one receiver antenna, two transmitter and M receiver antennas. In this section, two transmitter and receiver antennas are taken as an example to explain the encoding of *STBCs*. The input bit sequence is modulated, and mapped to one symbol in constellation which has 2^B symbols. The constellation is represented as a complex plane for example QPSK, PSK and PAM.

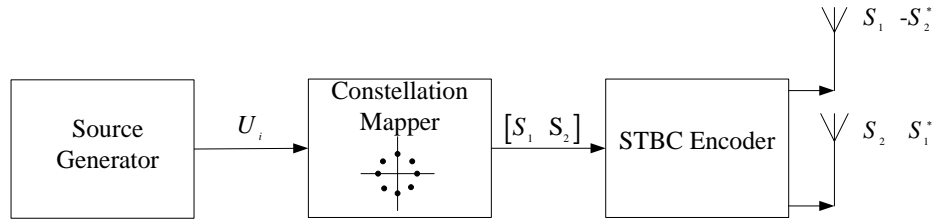


Figure 14 Transmitter diagram of orthogonal space-time block codes

The transmitter picks two symbols from the constellation diagram by using a block of $2B$ bits. Assume that the symbols are S_1 and S_2 , where S_1 is transmitted from the first antenna and S_2 is transmitted from the second antenna. Then, in the next time slot, the symbols $-S_2^*$ is transmitted from the first antenna and S_1^* is transmitted from the second antenna, where $(.)^*$ is denoted as the complex conjugate. The transmitted symbols are written as:

$$\begin{bmatrix} S_1 & -S_2^* \\ S_2 & S_1^* \end{bmatrix} \quad (3.5)$$

The reception and decoding of the signal depend on the number of the received antennas. In this example, two transmitted and received antennas are used. Therefore, the signal at the first receiver antenna RX_1 is:

$$\begin{aligned} y_{11} &= h_{11}s_1 + h_{12}s_2 + n_{11} \\ y_{12} &= -h_{11}s_2 + h_{12}s_1 + n_{12} \end{aligned} \quad (3.6)$$

While the signal at the second receiver antenna RX_2 is:

$$\begin{aligned} y_{21} &= h_{21}s_1 + h_{22}s_2 + n_{21} \\ y_{22} &= -h_{21}s_2 + h_{22}s_1 + n_{22} \end{aligned} \quad (3.7)$$

where y represents the received signal, h_{ij} represents the channel coefficients between the transmitter antenna i and receiver antenna j and n_{ij} is the AWGN.

3.3.2. MAP decoding of space-time block codes

Symbol-wise *Maximum A-Posteriori* (MAP) decoding rule for space-time block codes was introduced by Bauch in [27]. The soft outputs that obtained by the space-time MAP decoder can be used as input to channel decoders. The posteriori probabilities of the transmitted t -array symbols S_1, S_2, \dots, S_t , a symbol gives the received signal $y_{11}, \dots, y_{n2}, y_{21}, \dots, y_{mn}$ were expressed in [27] as:

$$p(s_1, \dots, s_t | y_{11}, \dots, y_{qn}) = p(y_{11}, \dots, y_{qn} | s_1, \dots, s_t) \cdot p(s_1, \dots, s_t) \quad (3.8)$$

where $p(S_1, \dots, S_t)$ is the a-priori information of the transmitted symbols which can be calculated from other independent source such as (the inner encoder in serial concatenated codes). Moreover, according to Bauch [22], the probability in (3.8) can be written over non-dispersive Rayleigh fading channels using:

$$p(y_{11}, \dots, y_{qn} | s_1, \dots, s_t) = \frac{1}{(\sigma\sqrt{2\pi})^{qn}} \exp \left\{ -\frac{1}{2\sigma^2} \sum_{l=1}^q \sum_{i=1}^n \left| y_{li} - \sum_{j=1}^p h_{lj} s_{ji} \right|^2 \right\} \quad (3.9)$$

where σ represents the noise variance, h_{ij} is the channel coefficient between the antenna i and received antenna j and S_1 is denoted as the transmission signal which is taken from the constellation diagram. For more clarity Alamouti with two transmitter and receiver antennas are taken as example, where $t=2$, $n=2$ and $p=2$. Hence, there is no priori information that is $p(S_1, \dots, S_t) = C$ where C is a constant number. To obtain the posteriori information from the received signal of the t -array symbols, the equations (3.8) and (3.9) are used in [22] as:

$$\begin{aligned} & p(s_1, \dots, s_t | y_{11}, \dots, y_{qn}) \\ &= C \cdot \exp \left\{ -\frac{1}{2\sigma^2} \sum_{l=1}^q \left[\left| y_{l1} - h_{l1}s_1 - h_{l2}s_2 \right|^2 + \left| y_{l2} + h_{l1}s_2 - h_{l2}s_1 \right|^2 \right] \right\} \end{aligned} \quad (3.10)$$

where $C' = C \cdot 1/(\sigma\sqrt{2\pi})^{qn}$. In order to obtain a general expression of the posteriori probability for the symbols S_1, S_2 , the related terms are ignored in the previous equation due to the orthogonality of the code. Where $|y_{l1}|^2$ and $|y_{l2}|^2$ are constant because they do not depend on S_2 and merged into the constant C' . The equation (3.8) simply rewritten as follows:

$$p(s_1 | y_{11}, \dots, y_{qn}) = C' \cdot \exp \left\{ -\frac{1}{2\sigma^2} \left[\left| \sum_{l=1}^q (h_{l1}^- y_{l1} + h_{l2}^- y_{l2}) - s_1 \right|^2 + \left(-1 + \sum_{l=1}^q \sum_{i=1}^2 |h_{li}|^2 \right) |s_1| \right] \right\} \quad (3.11)$$

Similarity, S_1 -related terms in equation (3.8) are eliminated and is simplified as

$$p(s_1 | y_{11}, \dots, y_{qn}) = C' \cdot \exp \left\{ -\frac{1}{2\sigma^2} \left[\left| \sum_{l=1}^q (h_{l2}^- y_{l1} - h_{l2}^- y_{l2}) - s_2 \right|^2 + \left(-1 + \sum_{l=1}^q \sum_{i=1}^2 |h_{li}|^2 \right) |s_2| \right] \right\} \quad (3.12)$$

The MAP decoding for other space time block codes schemes are given in [22].

3.4. Trellis Coded Modulation

In order to achieve reliable transmission over noisy channels, channel coding should be employed before transmission. The convolutional codes and block codes are two types of channel coding. These codes can obtain coding gain by adding redundancy to the bit stream. The ratio of the input bit sequence to the total output sequence is called the code rate R . The addition of the redundancy decrease the code rate R . This causes an increase in the bandwidth, which creates a problem in some bandwidth-limited communication systems. Trellis-coded modulation (TCM) has developed in recent years as a combination of coding and modulation for data transmission over noisy and band-limited channels. Trellis-coded modulation was first introduced by Ungerboeck in [8]. TCM solves the bandwidth problem without bandwidth expansion or without the reduction of the effective rate. For the decoding of TCM, a soft-decision maximum-likelihood decoder is used. On the other hand, the complexity of TCM decoding is higher than uncoded modulation.

3.4.1. Design of trellis coded modulation schemes

Ungerboeck introduced the redundancy required for error control without increasing the signal bandwidth. The general structure of TCM encoder and modulator is illustrated in Fig. 15. This operation can be explained as follow:

Assume m is the set of bits to be transmitted. One bit is added to the set of m bits. The constellation is extended from 2^m to 2^{m+1} . The $m + 1$ encoded blocks are used for the selecting from the extended signal constellation. In this case, the transmission rate is the same and there is no need for additional bandwidth. The main idea of TCM systems lies in the method to map m information bits into 2^{m+1} signals (extended constellation). This operation is called set partitioning. Set partitioning maximizes the Euclidian distance between symbols sequence.

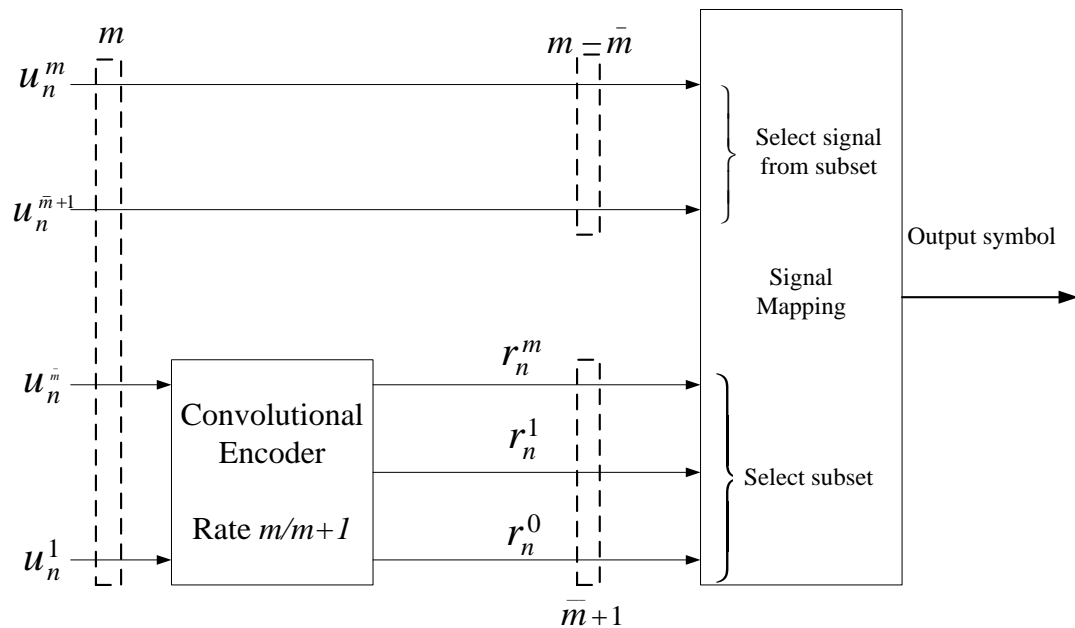


Figure 15 Trellis coded modulation procedure

The selection of the partitions is done by using a convolutional encoder. To clarify more, this operation is explained as follow:

M is defined as a number of bits in one symbol and \bar{M} is the number of bits after encoding operation by using convolutional encoder. The rate of this encoder is

$\bar{M}/\bar{M} + 1$. The overall length of the coded bits is $\bar{M} + 1$. These coded bits are used to select one symbol of the $2^{\bar{M}+1}$ partitions signals in constellations at the $\bar{M} + 1$ levels of the constellation partition tree. Then, the signal is selected from the chosen partition by using $\bar{M} - M$ bits. The convolutional encoder structure is used to determine the selected signal. Thus, the whole system is called trellis coded modulation.

3.4.2. Set partitioning

The digital modulated signal is represented by a constellation diagram, such as Quadrature Amplitude Modulation (QAM) and Phase-Shift Keying (PSK). There are three constellation diagrams. For example, rectangular constellations, one dimension constellations and Mary phase shift keying constellations. These constellations are different from each other in the minimum distance. The rectangular constellations have better Euclidian distance. However is suffered from distortion when they passed through the non-linear device. The MPSK although has Euclidian distance relatively small and it is not distorted. The 8-QPSK and 16-QPSK are illustrated in the following Fig. 16.

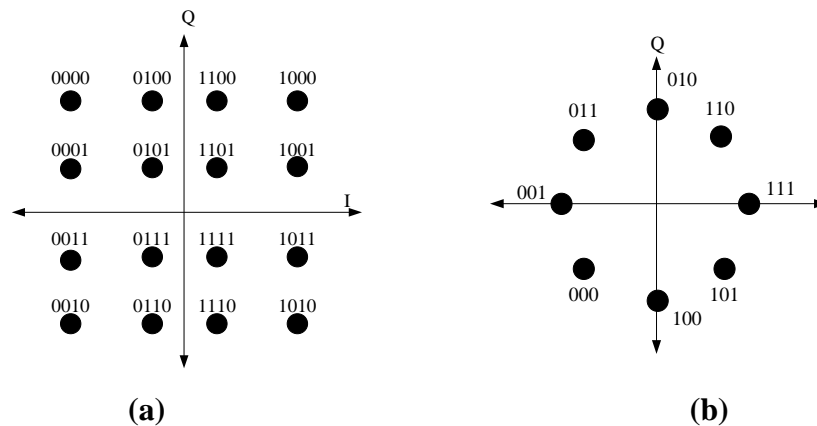


Figure 16 A constellation diagram. (a) rectangular 16-QAM (b) 8-PSK.

The set partitioning is an operation used for dividing the signal constellation diagram into subsets depending on the criteria of the larger Euclidian distance between points in constellation diagram. To clarify more the 8-PSK example is taken to illustrate the set partitioning operation as follows:

The constellation diagram A which consists of eight points is divided into two subsets G_1 and G_2 , each subset has four points. These subsets are divided into small subsets depending on the larger minimum distance, that is G_1 is divided into R_1 and R_2 , and G_2 is divided into R_3 and R_4 . At each subdivision operation, the Euclidian distance is greater than the Euclidian distance at the previous level. The 8-PSK example set partitioning is depicted in Fig. 17.

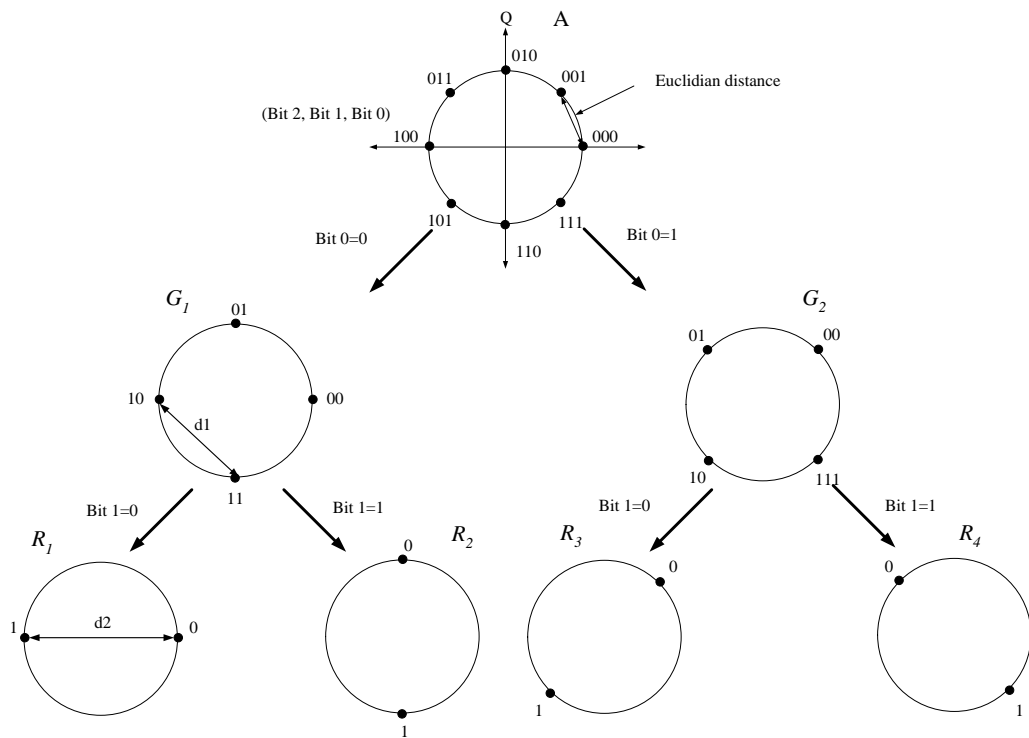


Figure 17 8-PSK set partitioning operation

3.4.3. Selection of the partitions

In TCM, the convolutional encoder is used for the selection of the signals. The convolutional encoder is divided into two categories, systematic and non-systematic convolutional encoders. The trellis diagram depends on the type of the convolutional encoder. If the systematic convolutional encoder is used, there are parallel transitions between states in the trellis diagram. If non-systematic convolutional encoder is used, there is no parallel transition in the trellis diagram. The TCM structure with

systematic convolutional encoder with rate 2/3 is seen in Fig. 18 where the expansion from 4-QPSK to 8-QPSK is done.

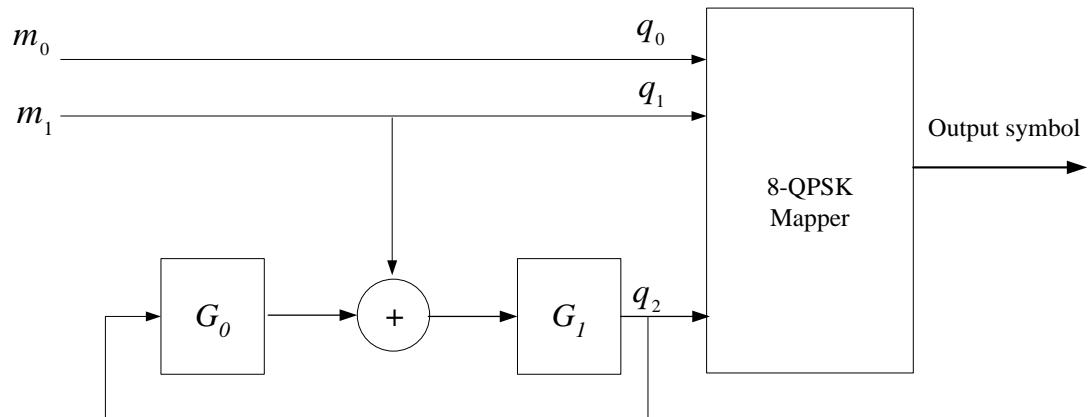


Figure 18 TCM with systematic convolutional encode with rate 2/3

Also, the trellis diagram of the above structure is shown in Fig. 19. Hence, the codewords are carefully chosen from the constellation diagram according to Ungerboeck design rule.

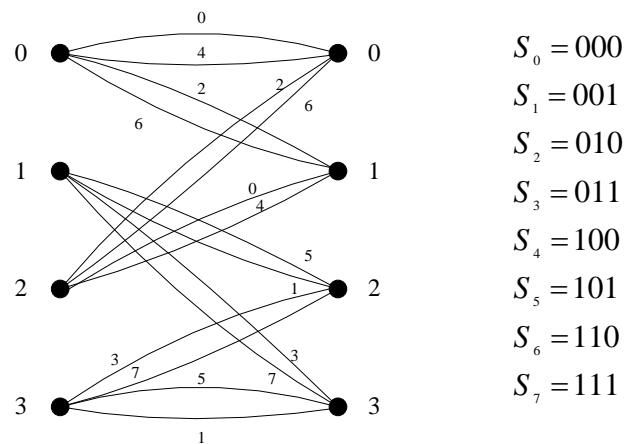


Figure 19 Trellis diagram of TCM with systematic convolutional

CHAPTER 4

LOW LATENCY JOINT COMMUNICATION STRUCTURES

In this chapter, new concatenated structures involving convolutional code product codes (CPCs) and space-time code (STCs) are introduced. Moreover, the idea is extended to a concatenated system structure involving CPCs and trellis coded modulation. The simulation results of these concatenated systems are also presented in this chapter.

4.1. Performances of CPCs, SCCCs, and PCCCs

In our simulation, we use recursive systematic convolutional code $(1,5/7)_{octal}$ for all constituent encoders. An S -random interleaver with separation distance ($S=17$) is utilized between the inner and outer encoders in SCCCs, between the upper and lower encoders in PCCCs and between the clusters in CPCs. In the concatenation structures SCCCs and PCCCs, the input sequence frame has a length 1024 bits. The encoded sequence is binary phase shift key (BPSK) modulated. The modulated signal is passed through an AWGN channel.

For CPCs encoding, we formed a matrix size 4×256 bits. N and M are the number of row decoders for the inner and the outer clusters. The encoded data matrix is multiplexed to a single stream vector and then BPSK modulated. At the receiver side, we use log-MAP decoders for iterative decoding purposes in SCCCs and PCCCs. In CPCs, we use separated log-MAP decoders. Moreover, we use 10 iterations for decoding. The simulation results of the above structures are seen in Fig. 20.

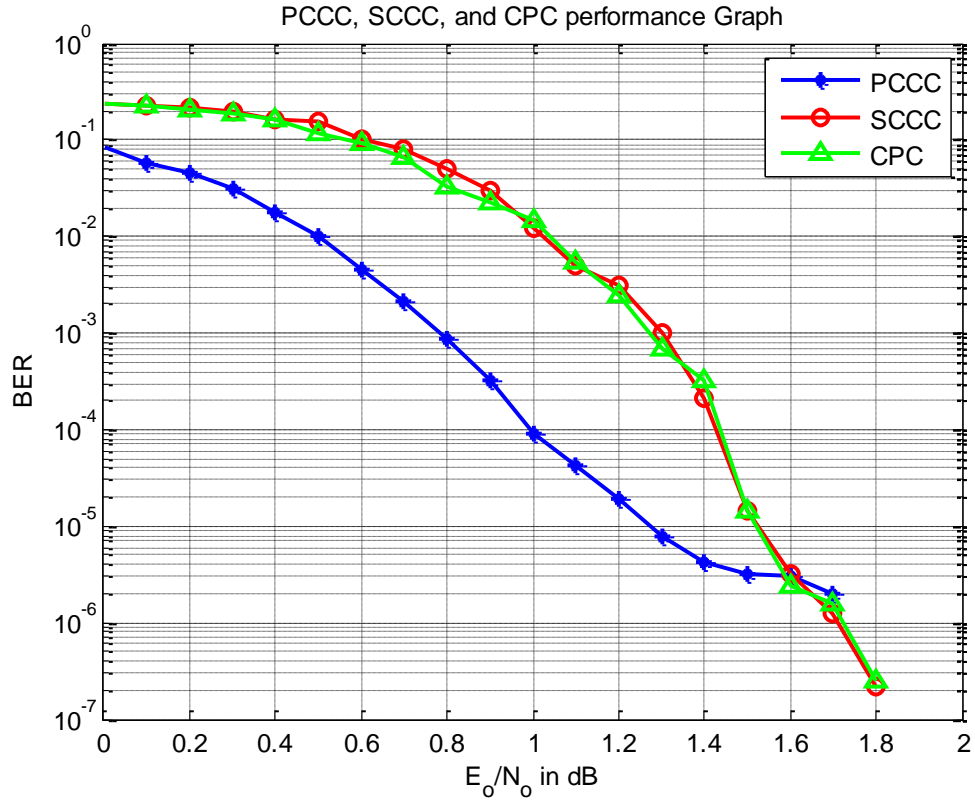


Figure 20 PCCC, SCCC and CPC performance graph

From the performance graph, we conclude that, PCCC has better performance than CPC and SCCC at very low E_b/N_0 levels. The PCCC performs worse at height E_b/N_0 level. Also, it is seen from the results that the performance of CPC is similar to the SCCC with fast decoding operation due to parallel processing.

4.2. CPC Joint Structure with STTCs

After putting the data into a matrix, the rows of the matrix are encoded separately by using the constituent codes, such as linear block codes or recursive systematic convolutional encoders, this represents the outer encoder. Then, the encoded rows are passed through a modulator to obtain symbol matrix, for example 4-PSK and 8-PSK, etc. Next, the modulated rows symbols are passed through space-time trellis encoder, such as Tarokh's 4-state and 8-state STTCs. Finally, the encoded symbols are multiplexed to a single vector to be transmitted using multi antennas. Serial to

parallel (S/P) and parallel to serial (P/S) converters are used in this concatenation structure. The whole encoding operation is seen in Fig. 21.

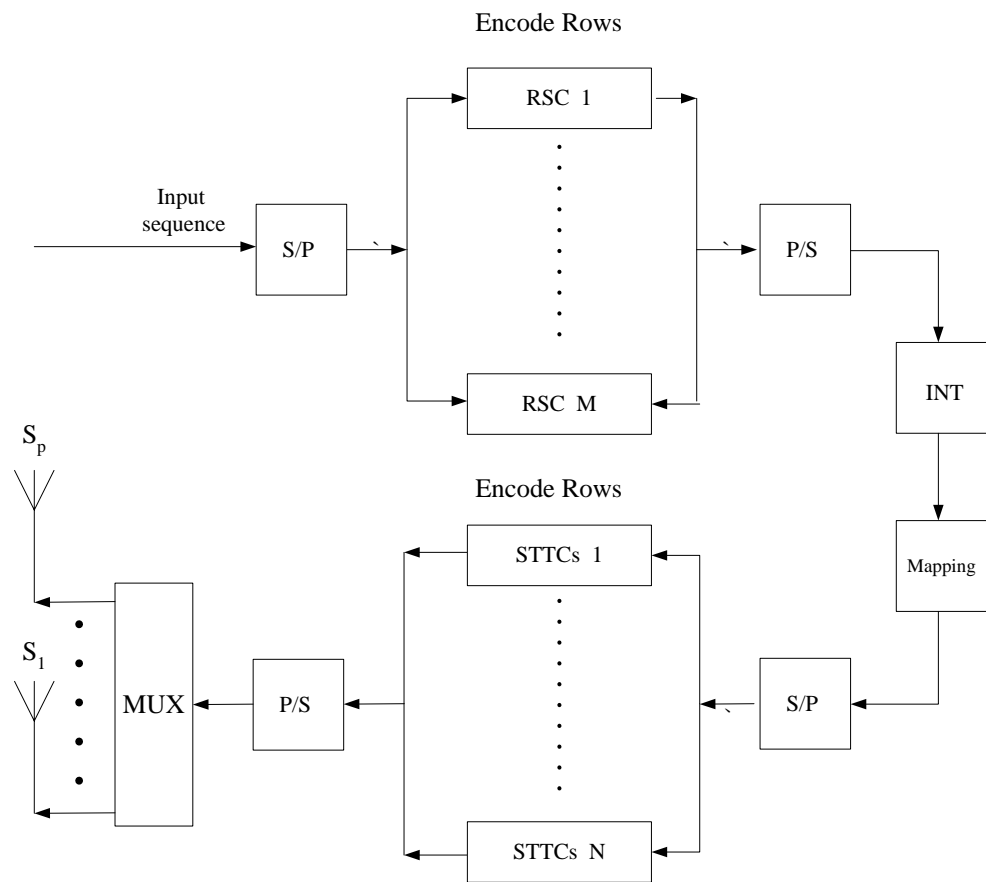


Figure 21 CPCs - STTCs encoding operation

As in Fig. 21, an interleaver is utilized between CPCs and STTCs to obtain a good performance. The signal is passed through *the Rayleigh fading channel*. At the receiver side, the received signal is decoded using symbol-wise MAP algorithm. On the other hand, bit-wise algorithm is used for CPCs decoding. Thus, *symbol probabilities to bit probabilities and bit to symbol probabilities* are needed to convert these probabilities.

4.2.1. Symbol to bit prob. / bit. to symbol prob. converter

This operation is needed when the decoders produce different probabilities. This operation is explained in the following example:

Let STTC uses 4-QPSK modulation, these symbols are denoted as S_0, S_1, S_2, S_3 which represent the bits pairs 00, 01, 10 and 11 respectively. In general, assume S_i represents the bit pairs $b_0 b_1$. The constellation diagram of 4-QPSK is depicted in Fig. 22.

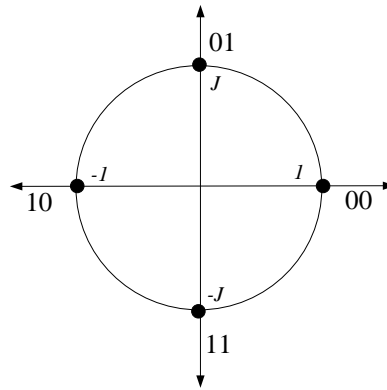


Figure 22 4-QPSK constellation diagram

The relation between bit and symbol probabilities in log-domain is written as:

$$\begin{aligned}
 p(b_0 = 0) &= p(S_0) + p(S_3) \\
 p(b_0 = 1) &= p(S_1) + p(S_2) \\
 p(b_1 = 0) &= p(S_2) + p(S_3) \\
 p(b_1 = 1) &= p(S_1) + p(S_0).
 \end{aligned}
 \tag{4.1}$$

The STTCs row decoders obtain the symbol probabilities, and then these probabilities are converted to bit probabilities using (4.1). These bit probabilities are sent to Bit-wise MAP row decoders. Rows decoders obtain the update bit probabilities. These updated bit probabilities are converted to symbol probabilities, which represent updated symbol probabilities. The relation between bits to symbol probabilities in log-domain is written as:

$$\begin{aligned}
p(s_0) &= p(b_0 = 0) + p(b_1 = 0) \\
p(s_1) &= p(b_0 = 1) + p(b_1 = 0) \\
p(s_2) &= p(b_0 = 1) + p(b_1 = 1) \\
p(s_3) &= p(b_0 = 0) + p(b_1 = 1).
\end{aligned}
\tag{4.2}$$

These probabilities are fed back to *STTCs* row decoders. The decoding operation is repeated for a sufficient number of iterations. The decoding operation of this structure is shown in Fig. 23

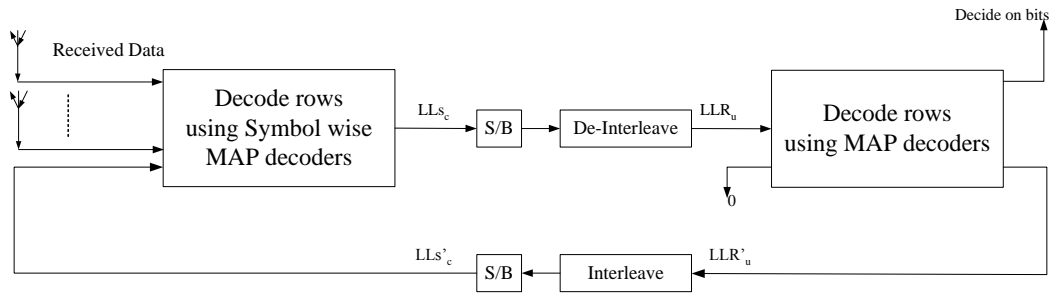


Figure 23 CPCs - STTCs decoding operation

4.3. Joint Structure Involving CPCs and STBCs

Encoding operation of this joint structure is similar to the joint structure involving CPCs and STTCs. The only difference of this structure is that at the inner encoders *STBCs* are used instead of *STTCs*. For *STBCs* encoders, different space-time block codes can be used such as Alamouti codes. The encoding operation of this structure is depicted in Fig. 24.

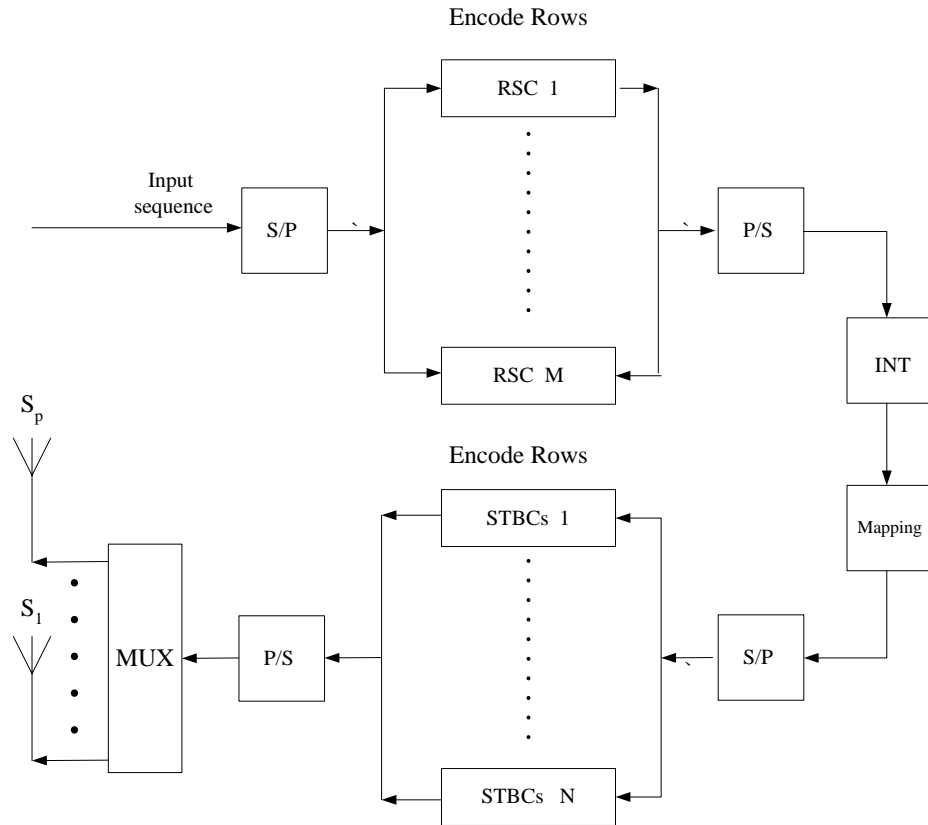


Figure 24 CPCs - STBCs encoding operation

For decoding of this joint structure, simple symbol-wise and bit-wise MAP algorithms are used for the decoding issues. In this structure, symbol-to-bit and bit-to-symbol converters are applied between STBCs and CPCs decoders. STBCs use simple symbol wise MAP decoding algorithm. The decoding operation is seen in Fig. 25.

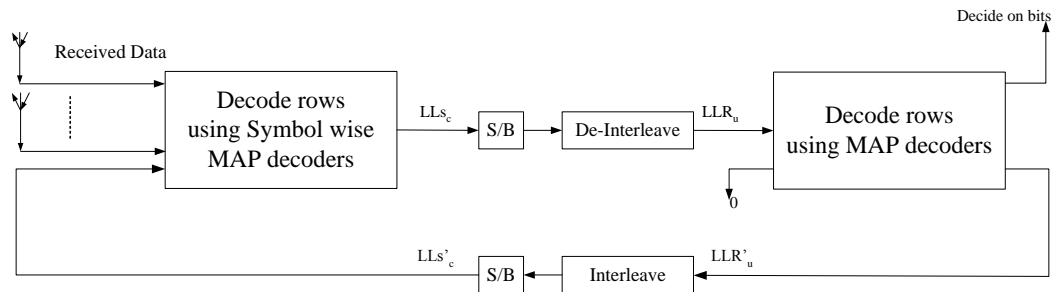


Figure 25 CPCs - STBCs decoding operation

4.4. Joint Structure Involving CPCs and TCM

TCM uses convolutional codes. The main idea of TCM lies on maximizing the Euclidian distance among the modulated signal. Since CPCs uses convolutional encoder which make it suitable to be integrated with TCM. In this joint structure, the outer encoder is similar to that one we used in CPCs. The only change in this structure is the inner encoder is replaced by TCM encoder. Each row of the matrix is encoded using Ungerboeck 8 or 4 states after being interleaved. The encoding operation is depicted in Fig. 26.

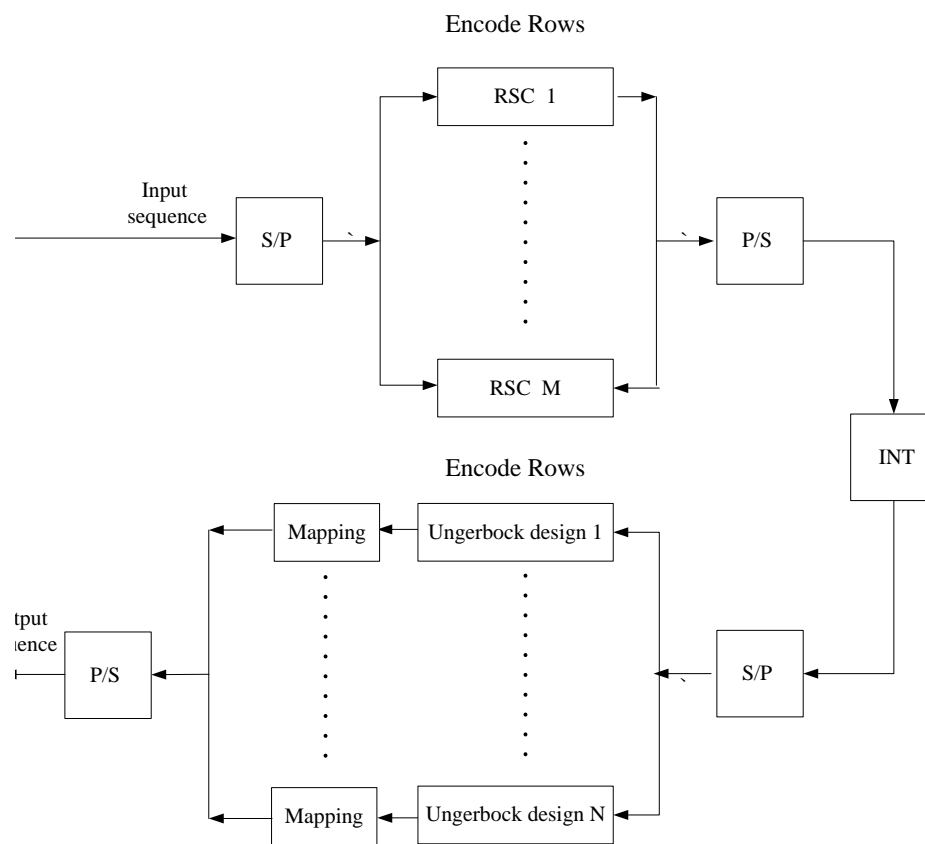


Figure 26 CPCs - TCM encoding procedure.

The decoding operation of the joint structure is more complex than the classical CPCs. Hence, Symbol-wise MAP algorithm is used for columns decoding. In addition, *symbol probabilities to bit probabilities and bit to symbol probabilities* are applied to convert the probabilities. The decoding operation is seen in Fig 27.

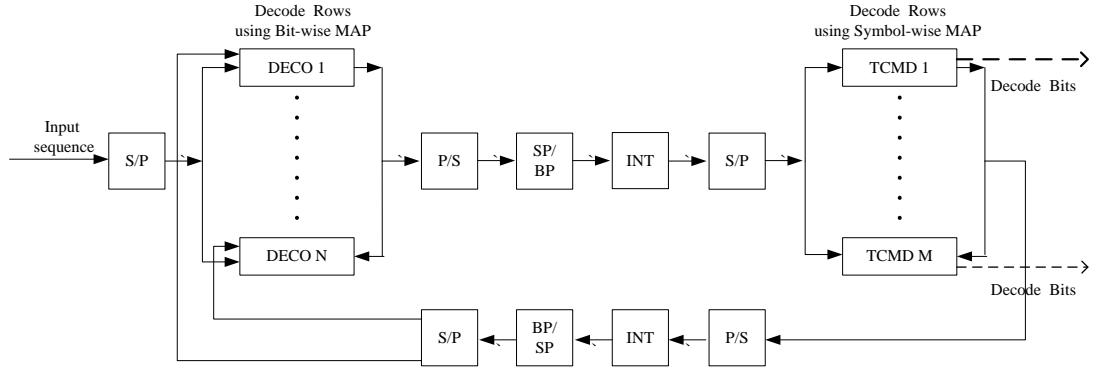


Figure 27 CPCs - TCM decoding operation.

4.5. Simulation Results of the Joint Structures

The simulation results are obtained by using C++ program. We used a data frame length of 1024 bits as an input for all our simulations. For all joint structures, the same outer CPCs encoders which have $(1, 5/7)_{octal}$ as component codes and the number of rows is fixed as 4. For the channel, Rayleigh distributed flat fading channel is employed and perfect channel information is assumed at the receiver side. Additionally, TCM joint structure simulation was tested under the AWGN channel.

4.5.1. Simulation results of CPCs and STTCs

CPCs encoders are used as outer encoder of this structure. The 4-QPSK modulation is used for mapping and Tarokh's 4-state STTC is used as the inner encoder. Moreover, we used *S-random* interleaver with ($S=17$) between CPCs and STTCs encoders. In this structure, two antennas are used at the transmitter and receiver side. Fig. 28, shows the performance of the concatenated system, the line in red represents RSCs and STTCs and the blue line represents CPCs and STTCs.

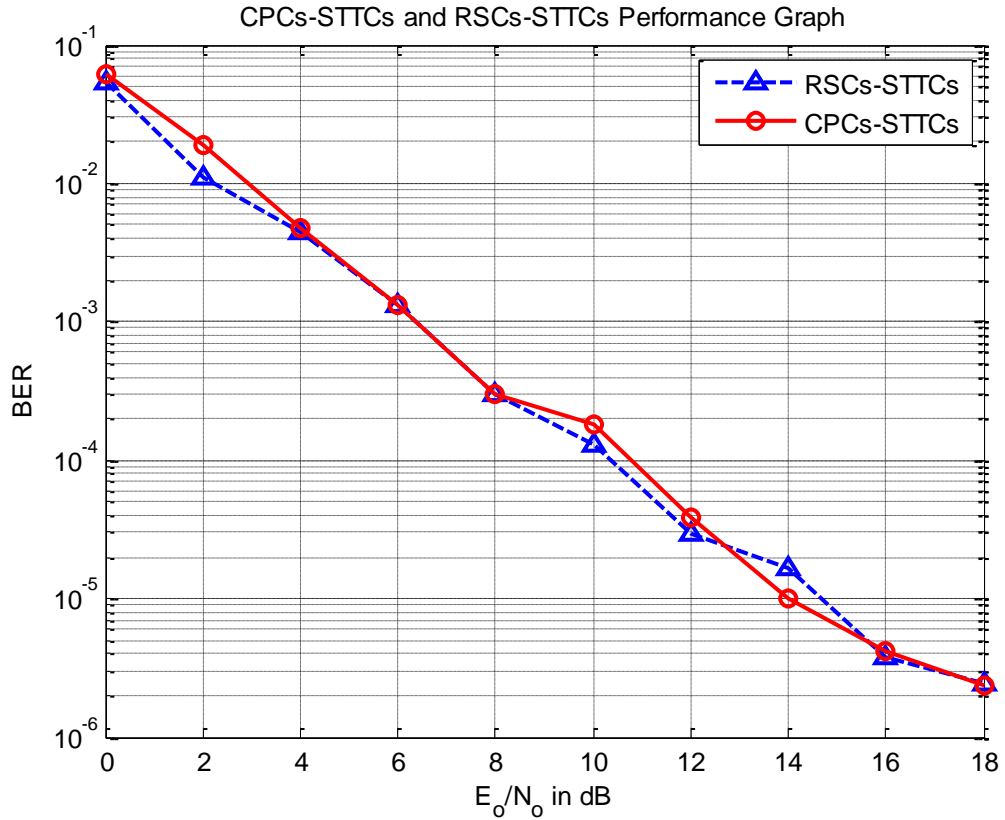


Figure 28 CPCs - STTCs and RSCs - STTCs performance graph

From Fig. 28, the proposed structure shows the same performance of the concatenation system (*RSCs*, *STTCs*) and has much low decoding latency due to the parallel processing.

4.5.2. Simulation results of CPCs and STBCs

For the second proposed structure CPCs and STBCs, we used the same CPCs encoders that are used with the previous structure and with the other factors. In this concatenated system, the inner encoders are replaced with STBCs. Alamouti code is used as inner encoder. The performance of the system is shown in Fig. 29.

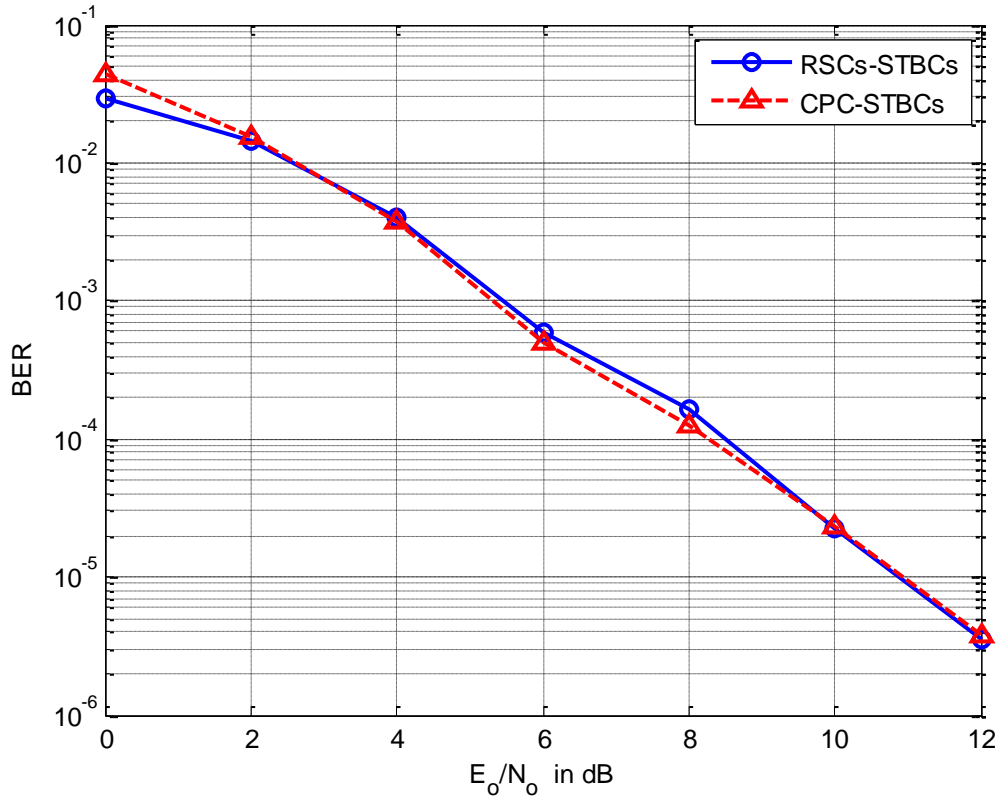


Figure 29 CPCs - STBCs and RSCs - STBCs performance graph

From Fig. 29, the performance of the concatenated system involving CPCs and STBCs is similar to the concatenated system involving RSCs and STBCs. Moreover, the proposed structure shows low decoding latency due to the parallel processing.

4.5.3. Simulation results of CPCs and TCM

In the simulation of CPCs and TCM, the outer encoder is chosen as in the the previous simulations. The inner encoder is replaced with 8-state Ungerboeck design. Ungerboeck 8-state encoder is depicted in Fig. 30. Single antenna is used at the transmitter and receiver sides; also, the simulation of this structure is done over AWGN channel.

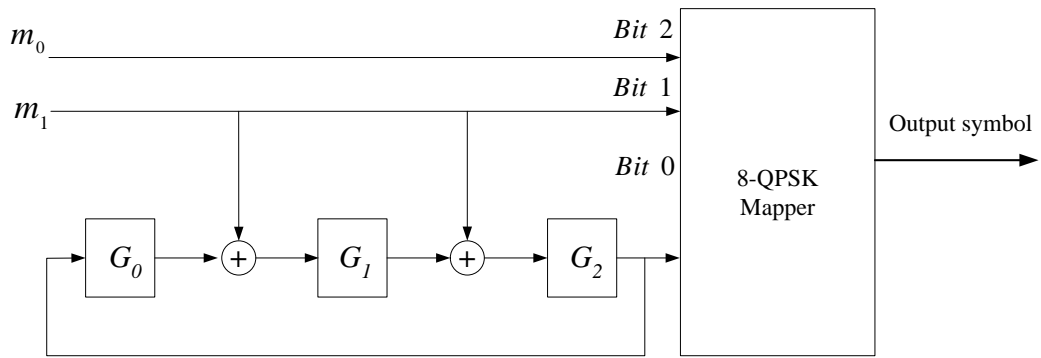


Figure 30 8-PSK TCM encoder

For the decoding of TCM symbol-wise and bit-wise MAP algorithms are used for CPCs and TCM decoding operations. The decoding iteration number is 8. Fig. 31 shows the performance of the concatenated system.

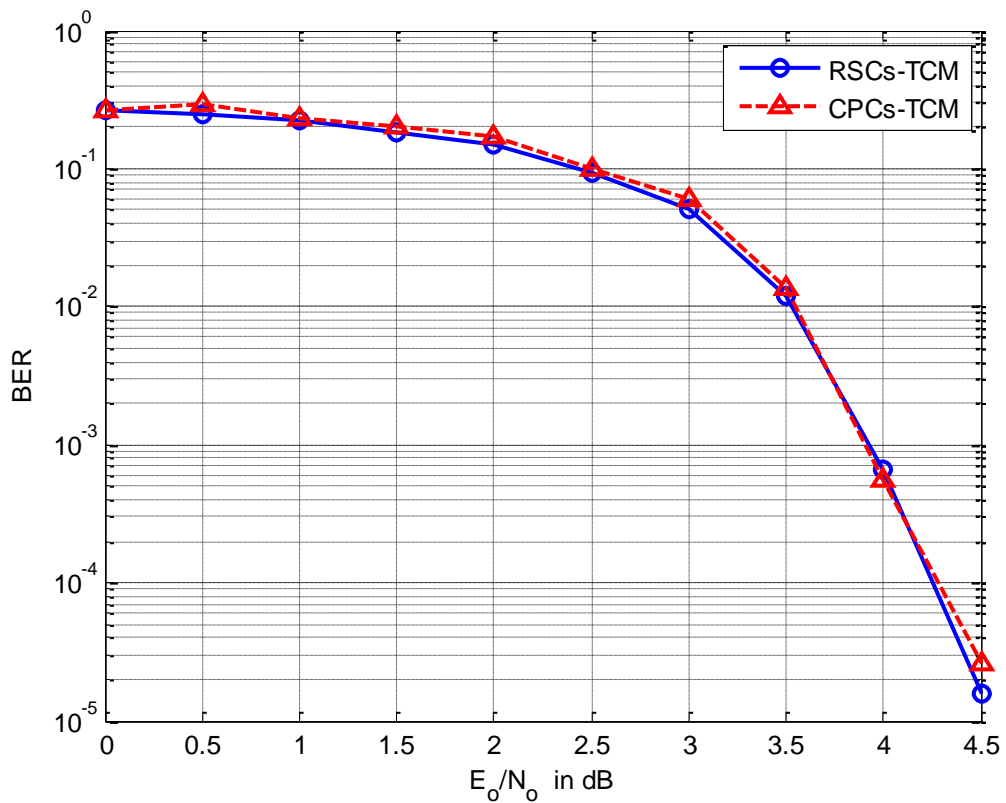


Figure 31 CPCs - TCM and RSCs - TCM performance graph

From the simulation results, we see that the performance of the proposed structure of CPCs and TCM is similar to RSCs and TCM with a high speed decoding

CHAPTER 5

CONCLUSION AND FUTURE WORK

5.1. Conclusion

The experiential results show that Turbo codes performance is very close to Shannon limits. Despite of the good performance of the turbo codes, iterative decoding operation and complex decoding algorithm reduce their attractiveness for practical implementations due to the large decoding latency. This thesis focused on enhancing of the decoding latency as well keeping the performance of the system same. In this thesis, we concentrate on a parallel processing method. We proposed parallel processing of serially concatenated systems, where the latency is reduced by using parallel processing operation. The latency of the concatenated systems is reduced by a factor, which represents the number of parallel processors utilized at the receiver side. In our work, we depend on the idea of the proposed structure of CPCs. This structure employs the parallel encoding operation at the transmitter side, which will be used at the receiver side for decoding. CPCs structure has a low decoding latency and shows the same performance of other counterparts. CPCs use convolutional codes as appropriate components and have time invariant trellis structure. Due to the advantage of CPCs, which made it highly suitable for integration issues, we proposed joint structures involving CPCs with space time code and CPCs with trellis code modulation (TCM). These proposed structures are iteratively decoded where bit and Symbol-wise MAP algorithms are used. The results of the simulations lead us to reach a new fact which states that the structures we introduced have low decoding latency obtained after applying parallel processing operation, and show the same performance compared to their counterparts. The new structures are spectrally efficient due to the use of multi-antenna. Finally, it has to be

mentioned that the parallel processing operation we used increased the hardware complexity due to multiple processors employed for the decoding of outer and inner units. Hereby, the costs of the new structures have risen dramatically.

5.2. Future work

In this work we proposed a new concatenated joint communication structures involving convolutional product codes, space time codes and trellis coded modulation. In future, these joint structures should be integrated with Orthogonal Frequency Division Multiplexing (OFDM). The implementation of these joint structures on a Field Programmable Gate Array (FPGA) platform should also be implemented.

REFERENCES

1. **Shannon C., (1948)**, “*A Mathematical Theory of Communication*”, Technology. Journal. Bell System, vol. 27, pp. 379-423.
2. **Hamming R. W., (1950)**, “*Error Detecting and Correcting Codes*”, Technology. Letter, Bell Systems, vol. 26, no. 2, pp. 147-160.
3. **Golay M., (1960)**, “*Notes on Digital Coding*”, Proceedings of IEEE, vol. 37, pp. 67.
4. **Bose R. C., Ray-Chaudhuri D. K., (1960)**, “*On A Class of Error Correcting Binary Group Codes*”, Information and Control, vol. 3, pp. 69-79.
5. **Reed I. S., Solomon G., (1960)**, “*Polynomial Codes Over Certain Finite Fields*”, Society for Industrial and Applied Mathematics (SIAM) Journal on Applied Mathematics, vol. 8, pp. 598-606.
6. **Elias P., (1955)**, “*Coding for Noisy Channel*”, Institute of Radio Engineers. Record, vol. 4, pp. 37-47.
7. **Viterbi A. J., (1967)**, “*Error Bound for Convolutional Codes and an Asymptotically Optimum Decoding Algorithm*”, IEEE Transaction. Information. Theory, vol. 13, pp. 260-269.
8. **Ungerboeck G., Csajka I., (1976)**, “*On Improving Data-Link Performance by Increasing the Channel Alphabet and Introducing Sequence Coding*”, IEEE Symposium. Inform. Theory, Romney, Sweden, pp.132- 140.
9. **Wicker S., (1995)** “*Error Control Systems for Digital Communications and Storage*”, Prentice Hall, Sweden, pp. 201-205.

10. **Forney, J. G. D., (1966)**, “*Concatenated codes*”, MA, USA: Massachusetts Institute of Technology (M.I.T). Press, pp.10-19.
11. **Berrou C, Glavieux A., Thitimajshima P., (1993)**, “*Near Shannon Limits Error-Correcting Coding and Decoding: Turbo-Codes*”, in Proc. International Conference on Communication (ICC’93), Geneva, Switzerland, pp.1064–1047.
12. **Franz V., Anderson J. B., (1998)**, “*Concatenated Decoding with A Reduced Search Based BCJR Algorithm*”, IEEE J. select. Areas Commun, vol.16, pp. 186-195.
13. **Lee D., Park T., (2005)**,“ *A Low Complexity Stopping Criterion for Iterative Turbo Decoding*”, Institute of Electronics, Information and communication Engineers (IEICE) Transactions. Communication, vol. 88, pp. 399-401.
14. **Zhai F., Fair I., (2003)**, “*Techniques for Early Stopping Error Detection in Turbo Decoding*”, IEEE Transactions. Communications, vol. 51, no.10, pp. 1617-1623.
15. **Jung J. W., Choi D. G., (2005)**, “*Design and Architecture of Low-Latency High-Speed Turbo Decoders*”, Electronics and Telecommunications Institute (ETRI) Journal, vol. 27, no. 5, pp. 525-532.
16. **Barbulescu S, A, (1996)**, “*Iterative Decoding of Turbo Codes and Other Concatenated Codes*”, Philosophiae Doctor, Univ. of South Australia, pp.24-31.
17. **Lin Y., Line S., Fossorier M., (1998)**, “*MAP Algorithm For Decoding Linear Block Codes Based on Sectionalized Trellis Diagrams*”, on Proceedings Global Communications 98, Sydney, Australia, pp. 201-212.
18. **Hsu J., Wang C., (1998)**, “*A Parallel Decoding Scheme for Turbo Codes*”, in Proceedings. International Symposium on Circuits and Systems (ISCAS) 98, pp. 445-448.

19. **Yoon S., Bar-Ness Y., (2002)**, “*A Parallel MAP Algorithm for Low Latency Turbo Decoding*”, IEEE Communications. Letter, vol. 6, no. 7, pp. 288-290.
20. **Wang Y., Zhang J., Fossorier M. and Yedidia J. S., (2005)**, “*Reduced Latency Turbo Decoding*”, in Signal Processing Advances in Wireless Communications, IEEE 6th workshop, Honolulu, USA, pp. 23-30.
21. **Benedetto S., Divsalar D., Montosi G., Pollara F., (1996)**, “*A Soft-Output Maximum A Posteriori (MAP) Module to Decoded Parallel and Serial Concatenated Codes*”, Jet Propulsion Laboratory (JPL) progress Report, pp. 123-130.
22. **Robertson P., Villebrum E., Hoehner P.(1995)**, “*A Comparison of Optimal and Sub-Optimal MAP Decoding Algorithms Operating in Log Domain*”, In IEEE. Conference. On Communications, vol. 2, pp.864-876.
23. **Host S., (1999)**, “*On Woven Convolutional Codes*”, Philosophiae Doctor, vol.9, Lund University, Sweden, pp. 7-16.
24. **Chaoui S., (2003)**, “*Convolutional Coupled Codes*”, Philosophiae Doctor, University of Darmstadt, Germany, pp. 44- 50.
25. **Gazi O., Yilmaz A. O., (2006)**, “*Turbo Product Codes Based on Convolutional Codes*”, Electronics and Telecommunications Research Institute (ETRI) journal, vol. 28, no. 4, pp. 453-460.
26. **Tarokh V., Seshadri N., Calderbank A. R., (1998)**, “*Space –Time Codes for High Data Rate Wireless Communication: Performance Criteria and Code Construction*”, IEEE Transactions information. Theory, vol. 44, pp.744-765.
27. **Bauch G., (1999)**, “*Concatenation of Space –Time Block Codes and Turbo-TCM*”, Proceedings. Of International Conference on Communications, pp. 1202 -1206.
28. **Zhipei C., Zhongfeng W., Parhi K., (2000)**, “*Iterative Decoding of Space-Time Trellis Codes and Related Implementation Issues*”, Pacific Grove, USA, pp. 562-566.

29. **Lin S., Costello D. J., (2004)**, “*Error Control Coding*”, prentice Hall. USA, pp. 78-88.

30. **Vucetic B., Yuan J., (2004)**, “*Turbo Codes Principles and Applications*”, Kluwer Academic Publishers, Spain, pp.502-511.

31. **Wesel R. D., (2003)**, “*Convolutional Codes*”, Encyclopedia of Telecommunications, vol. 1, pp.598-606.

32. **Elias P., (1954)**, “*Error Free Decoding*”, Institute of Radio Engineers Transaction. Information, Theory, vol. IT-4, pp.29-37.

33. **Benedetto S., Montorsi G., (1996)**, “*Unveiling Turbo Codes: Some Results on Parallel Concatenated Coding Schemes*”, IEEE Transaction. Information. Theory, vol. 42, no. 2, pp. 409-428.

34. **Benedetto S., Divsalar D., Montorsi G., Pollara F., (1998)**, “*Serially Concatenation of Interleaved Codes: Design and Performance Analysis*”, IEEE Transaction. Information. Theory, vol. 44, pp. 909-926.

35. **Fragouli C., Wesel R. D., (1999)**, “*S-Random Interleaver Design Criteria*”, IEEE Global Communications. vol. 5, pp. 2352-2356.

36. **Rankin D., Gulliver T. A., (2001)**, “*Single Parity Check Product Codes*”, IEEE Transaction. Communications, vol. 49, no. 8, pp. 1354-1362.

37. **Alamouti S., (1998)**, “*A Simple Transmitter Diversity Technique for Wireless Communications*”, IEEE Journal on Selected Areas in Communications (JSAC), vol. 16, pp. 1451-1458.

38. **Tarokh V., Jafarkhani H., (1999)**, “*Space-Time Block Codes From Orthogonal Designs*”, IEEE Transaction on Information Theory, vol.16,pp. 1456-1467.

APPENDICES A

CURRICULUM VITAE

PERSONAL INFORMATION

Surname, Name: AL-KATTAN, Ahmed Amer

Date and Place of Birth: 19 July 1989, Iraq

Marital Status: Single

Phone: 00905392091195

Email: eng_ahmed_katan@yahoo.com



EDUCATION

Degree	Institution	Year of Graduation
M.Sc.	Çankaya University, Electronics and Communications Engineering	2014
B.Sc.	University of Mosul/ College of /Electronics/ Communication Department	2010
High School	Mutamizeen High School	2007

WORK EXPERIENCE

Year	Place	Enrollment
2011- Present	Nokia Siemens Network (NSN) and Huawei.	Site Engineer

FOREIGN LANGUAGES

Arabic Mother Language, advanced English, beginner Turkish.

PUBLICATIONS

1. A. Amer, O. Gazi,” Joint structures for Convolutional Product and Space Time Trellis Codes”, *Mühendislik ve Teknoloji Sempozyumu*, Çankaya Üniversitesi, Ankara, 15 March, 2014.

HOBBIES

Football, Reading Books, Traveling